DETERMINATION OF TWO-DIMENSIONAL

ELASTIC THERMAL STRESS

A THESIS

Presented to

The Faculty of the Graduate Division

by

Frank Hughes Smith, Jr.

In Partial Fulfillment

of the Requirements for the Degree

Master of Science in Mechanical Engineering

Georgia Institute of Technology

May 1964

DETERMINATION OF TWO-DIMENSIONAL

ELASTIC THERMAL STRESS

Approved:

John H. Murphy

Kenneth R. Purdy

Charles E. Stoneking

Date Approved by Chairman: _May 26, 1964_

ACKNOWLEDGMENTS

The author wishes to express his deep appreciation to those many individuals who assisted in the completion of this work with their time and encouragement. Dr. John H. Murphy, who suggested the problem and served as faculty adviser, contributed much of his valuable time in advice and assistance. Appreciation is extended to Dr. Kenneth R. Purdy and Dr. Charles M. Stoneking for reviewing this work.

Special thanks are due Mr. George H. Pope, Chief of the Engineering Support Facility, ARO, Inc. for his encouragement and his staff for their assistance in the review and drafting of the work.

This work is affectionately dedicated to Beverly, Scott, and Jean, without whose love and patience it would not have been possible.

TABLE OF CONTENTS

LIST OF ILLUSTRATIONS

SUMMARY

During this study, various methods of calculating and
measuring thermal stresses were investigated for the particu-
lar case of a thermally loaded, thin, rectangular plate with
no edge restraint. Two approximate analytical solutions were
examined and solved for this case: one by the method of
Heldenfels and Roberts and one by a finite-difference method.
A high-speed digital computer was used for both solutions be-
cause of the numerous, repetitive calculations.

In conjunction with the analytical solutions, an
experimental investigation was conducted on a mild steel
plate of 1/4-inch thickness with a temperature gradient
imposed upon it. The stress values in the plate were calcu-
lated from strain measurements obtained from temperature-
compensated strain gages mounted on the plate and oriented
to measure both longitudinal and transverse strains. The
computer solutions were solved for a temperature difference
of 100^OF. The experimental data were taken for a temperature
difference across the plate of 50^OF. It was intended to be a
100° difference, but the edge cooling proved to be inadequate
and it could not be maintained. Since the elastic strain of
the material is a direct function of the temperature, the
analytical calculations were proportionately reduced for
comparison with the experimental data. Curves of longitudinal,

transverse, and shear stress are presented for both analytical solutions. Curves are also presented for the experimental stress values and are compared with the analytical values. A discussion of the relative merits of the analytical solutions is made, and estimates of their accuracy are included.

CHAPTER I

INTRODUCTION

The problem considered in this investigation is the determination of two-dimensional thermal stresses in the elastic range of metals. The present state of mechanical design frequently involves high local temperatures and resulting temperature or thermal gradients. It does not matter whether the temperatures are a direct result of a quest for higher efficiencies or an undesirable effect of supersonic flight, the thermal stresses generated by the temperature gradients must be accounted for in the final design.

The purpose of this study is to investigate and evaluate analytical solutions for thermal stresses and compare the analytical results with experimentally determined thermal stresses.

The equations of two-dimensional thermal stress were developed and are presented in general form. Two analytical solutions were investigated and applied to a selected specific case. Since the equations for the analytical solutions were involved and lengthy, they were programmed for solution by digital computer. The analytical results for the specific case are presented along with the experimentally determined

results. The results are discussed with conclusions and recommendations arrived at from the analysis.

CHAPTER II

THE TWO-DIMENSIONAL PROBLEM

The equations for the stress and strain distribution in a body are obtained from the following physical consider- ations: the stress-strain relationship for the material, the equilibrium of the body, and the geometry of deformation. These relationships are combined in the following manner after Timoshenko and Goodier[1] to give the desired general differ- ential expression.

A. Stress-strain relationship from Hooke's Law:

1. $\epsilon x = 1/E \left[\sigma x - \nu(\sigma y)\right]$ Strain in x direction

2. $\epsilon y = 1/E \left[\sigma y - \nu(\sigma x)\right]$ Strain in y direction

3. $\gamma xy = 1/G \ \tau xy = 2/E(1 + \nu)\tau xy$ Strain in xy direction

To include thermal strain:

1A. $\epsilon x = 1/E \left[\sigma x - \nu(\sigma y)\right] + \alpha T$

2A. $\epsilon y = 1/E \left[\sigma y - \nu(\sigma x)\right] + \alpha T$

B. Condition of equilibrium of the body:

1. $\dfrac{\partial \sigma x}{\partial x} + \dfrac{\partial}{\partial y} \tau xy = 0$

2. $\dfrac{\partial \sigma y}{\partial y} + \dfrac{\partial}{\partial x} \tau xy = 0$

C. Geometry of deformation:

1. $\epsilon x = \dfrac{\partial u}{\partial x}$ 　　　　　　　Strain in x direction

2. $\epsilon y = \dfrac{\partial v}{\partial y}$ 　　　　　　　Strain in y direction

3. $\gamma xy = \dfrac{\partial u}{\partial y} + \dfrac{\partial v}{\partial x}$ 　　　　Strain in xy direction

　　　　　　　　　　　　　　　　　　　or shear strain

Differentiating C_1 twice with respect to y gives:

$$\frac{\partial^2 \epsilon x}{\partial y^2} = \frac{\partial^3 u}{\partial x \partial y^2}$$

Differentiating C_2 twice with respect to x gives:

$$\frac{\partial^2 \epsilon y}{\partial x^2} = \frac{\partial^3 v}{\partial x^2 \partial y}$$

Differentiating C_3 with respect to x and y gives:

$$\frac{\partial^2 \gamma xy}{\partial x \partial y} = \frac{\partial^3 u}{\partial x \partial y^2} + \frac{\partial^3 v}{\partial x^2 \partial y}$$

As the three strains are all expressed in terms of u and v, they may be combined to give the following expression:

$$\frac{\partial^2 \gamma xy}{\partial x \partial y} = \frac{\partial^2 \epsilon x}{\partial y^2} + \frac{\partial^2 \epsilon y}{\partial x^2}$$

which is known as the Equation of Compatibility.

Satisfying all of the above relationships can be reduced to the solution of a single differential equation in the following manner.

Operating on the Equations of Equilibrium:
Differentiating B_1 with respect to x gives:

$$\frac{\partial^2 \sigma x}{\partial x^2} + \frac{\partial^2 \tau xy}{\partial x \partial y} = 0$$

Differentiating B_2 with respect to y gives:

$$\frac{\partial^2 \sigma y}{\partial y^2} + \frac{\partial^2 \tau xy}{\partial x \partial y} = 0$$

As both equations are equal to zero, adding them together gives:

$$\frac{\partial^2 \sigma x}{\partial x^2} + 2\frac{\partial^2}{\partial x \partial y}\tau xy + \frac{\partial^2 \sigma y}{\partial y^2} = 0$$

Solving for $[\partial^2/(\partial x \partial y)]\tau xy$ gives:

$$\frac{\partial^2}{\partial x \partial y}\tau xy = -\frac{1}{2}\left[\frac{\partial^2 \sigma x}{\partial x^2} + \frac{\partial^2 \sigma y}{\partial y^2}\right]$$

Substituting stress-strain relationship, equations 1A and 1B, into the Equation of Compatibility gives:

$$\frac{\partial^2 \gamma xy}{\partial x \partial y} = \frac{\partial^2}{\partial y^2}\left[\frac{1}{E}(\sigma x - \nu \sigma y) + \alpha T\right] + \frac{\partial^2}{\partial x^2}\left[\frac{1}{E}(\sigma y - \nu \sigma x) + \alpha T\right]$$

$$\frac{\partial^2 \gamma xy}{\partial x \partial y} = \frac{\partial^2}{\partial x \partial y}\left(\frac{1}{G}\tau xy\right) = \frac{\partial^2}{\partial x \partial y}\left[\frac{2}{E}(1 + \nu)\tau xy\right]$$

$$\frac{\partial^2}{\partial x \partial y}\left[\frac{2}{E}(1 + \nu)\tau xy\right] = \frac{\partial^2}{\partial y^2}\left[\frac{(\sigma x - \nu \sigma y) + E\alpha T}{E}\right]$$

$$+ \frac{\partial^2}{\partial x^2}\left[\frac{(\sigma y - \nu \sigma x) + E\alpha T}{E}\right]$$

$$\frac{2}{E}(1 + \nu) \frac{\partial^2}{\partial x \partial y} \tau xy = \frac{\partial^2}{\partial y^2} \left[\frac{(\sigma x - \nu \sigma y) + E\alpha T}{E} \right]$$

$$+ \frac{\partial^2}{\partial x^2} \left[\frac{(\sigma y - \nu \sigma x) + E\alpha T}{E} \right]$$

Substituting from the combined Equations of Equilibrium for

$$(1 + \nu) \left[-\left(\frac{\partial^2 \sigma x}{\partial x^2} + \frac{\partial^2 \sigma y}{\partial y^2} \right) \right] = \frac{\partial^2}{\partial y^2} \left[(\sigma x - \nu \sigma y) + E\alpha T \right]$$

$$+ \frac{\partial^2}{\partial x^2} \left[(\sigma y - \nu \sigma x) + E\alpha T \right]$$

Simplifying gives:

$$\frac{\partial^2 \sigma x}{\partial x^2} + \frac{\partial^2 \sigma y}{\partial x^2} + \frac{\partial^2 \sigma x}{\partial y^2} + \frac{\partial^2 \sigma y}{\partial y^2} + E\alpha \left(\frac{\partial^2 T}{\partial x^2} + \frac{\partial^2 T}{\partial y^2} \right) = 0$$

$$\left(\frac{\partial^2}{\partial x^2} + \frac{\partial^2}{\partial y^2} \right)(\sigma x + \sigma y) + E\alpha \left(\frac{\partial^2}{\partial x^2} + \frac{\partial^2}{\partial y^2} \right) T = 0$$

Defining the Airy stress function ϕ so that:

$$\sigma x = \frac{\partial^2 \phi}{\partial y^2} \qquad \sigma y = \frac{\partial^2 \phi}{\partial x^2} \qquad \tau xy = -\frac{\partial^2 \phi}{\partial x^2 y}$$

And substituting into the preceding expression gives:

$$\left(\frac{\partial^2}{\partial x^2} + \frac{\partial^2}{\partial y^2}\right)\left(\frac{\partial^2}{\partial y^2} + \frac{\partial^2}{\partial x^2}\right)\phi + E\alpha\left(\frac{\partial^2}{\partial x^2} + \frac{\partial^2}{\partial y^2}\right)T = 0$$

$$\left(\frac{\partial^4}{\partial x^4} + 2\frac{\partial^4}{\partial x^2 \partial y^2} + \frac{\partial^4}{\partial y^4}\right)\phi + E\alpha\left(\frac{\partial^2}{\partial x^2} + \frac{\partial^2}{\partial y^2}\right)T = 0$$

$$\nabla^4\phi + E\alpha\nabla^2 T = 0$$

which is the general differential expression for which a solution must be obtained.

The exact solution of the two-dimensional problem is the function ϕ that satisfies the differential equation and the required boundary conditions. It can be shown that for plane stress problems, ϕ must satisfy the following conditions at the boundary:

$$\frac{\partial^2\phi}{\partial y^2}\frac{dy}{ds} + \frac{\partial^2\phi}{\partial x\partial y}\frac{dx}{ds} = \overline{X}$$

$$\frac{\partial^2\phi}{\partial x^2}\frac{dx}{ds} + \frac{\partial^2\phi}{\partial x\partial y}\frac{dy}{ds} = -\overline{Y}$$

where $\overline{X}$ and $\overline{Y}$ are the x and y components of boundary loading and s is the arc length along the boundary.

2. The plate is unrestrained in all directions and there are no external loads on it so that all stresses are the result of the temperature gradient.

3. The plate is thin and is considered to be in a state of plane stress.

4. All stresses are within the elastic range and material properties are invariant with temperature.

5. All compressive stresses are sufficiently small to avoid elastic instability.
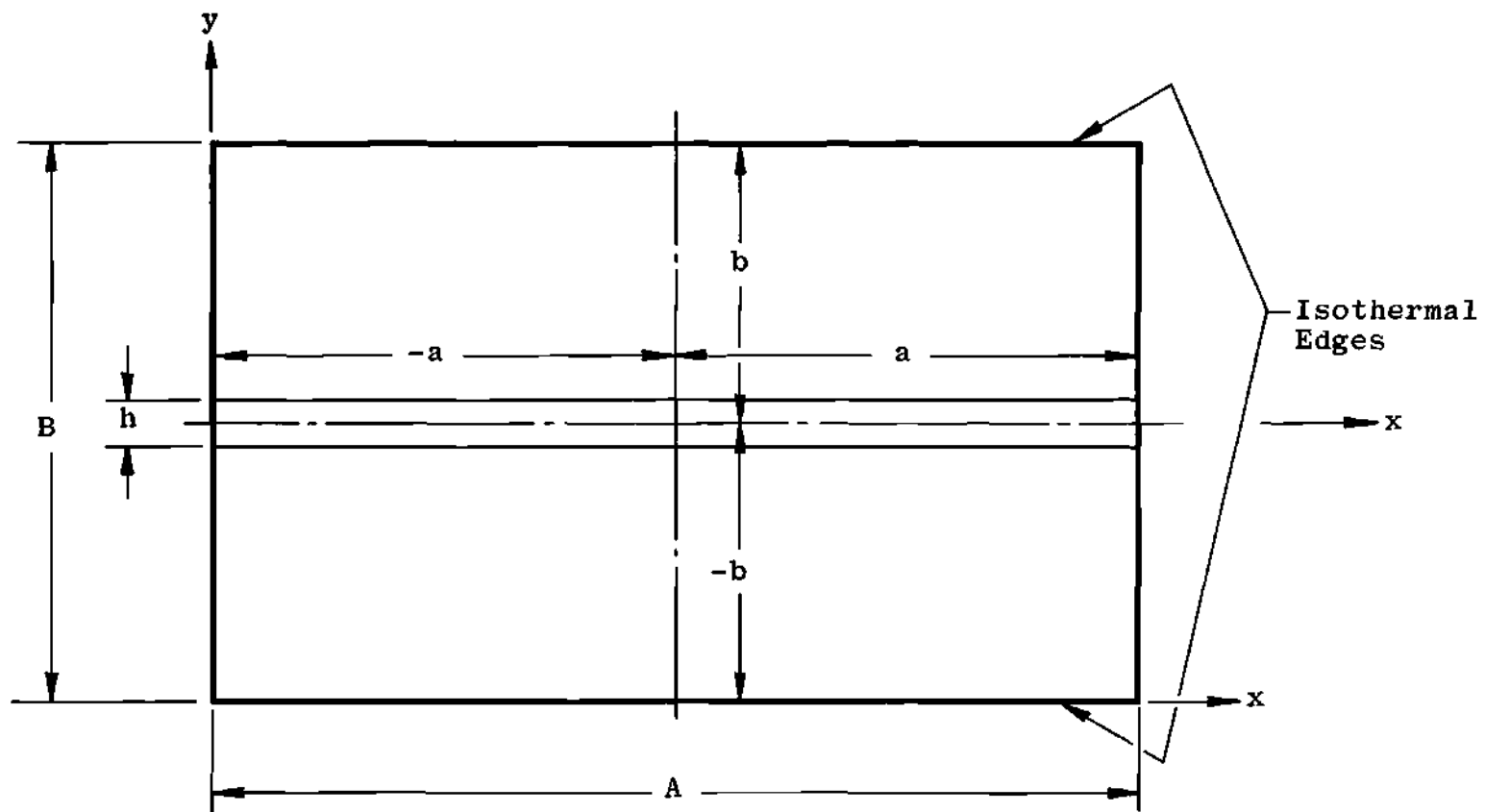
Figure 1.   Configuration of Rectangular Plate

$$U = \frac{1}{2E} \int_{-a}^{a} \int_{-b}^{b} \left[\sigma x^2 + \sigma y^2 - 2\mu \sigma x \sigma y + 2(1 + v)\tau xy^2 \right.$$

$$\left. + 2E\alpha T(\sigma x + \sigma y) \right] dxdy$$

where a and b are the half-length and half-width of the plate, respectively. By applying the boundary conditions for the specific problem of the rectangular plate to this equation, the functions f and g are determined where

$$g = \frac{b^2}{12} \left[1 - 3(y/b)^2 + 2(y/b)^3 \right]$$

and

$$f = E\alpha \, T_1 \, (1 + C_1 \sinh K_1 x \sin K_2 x + C_2 \sinh K_1 x \cos K_2 x$$

$$+ C_3 \cosh K_1 x \sin K_2 x + C_4 \cosh K_1 x \cos K_2 x)$$

where

$$K_1 = \sqrt{\frac{21 + \sqrt{1365}}{13b^2}}$$

and

$$K_2 = \sqrt{\frac{-21 + \sqrt{1365}}{13b^2}}$$

The constants of integration are determined to be:

$$C_1 = \frac{K_1 \sinh K_1 a \cos K_2 a - K_2 \cosh K_1 a \sin K_2 a}{K_1 \sin K_2 a \cos K_2 a + K_2 \sinh K_1 a \cosh K_1 a}$$

$$C_2 = C_3 = 0$$

$$C_4 = -\frac{K_1 \cosh K_1 a \sin K_2 a + K_2 \sinh K_1 a \cos K_2 a}{K_1 \sin K_2 a \cos K_2 a + K_2 \sinh K_1 a \cosh K_1 a}$$

$$C_5 = C_1 K_2 + C_4 K_1$$

$$C_6 = C_1 K_1 - C_4 K_2$$

$$C_7 = C_1 (K_1^2 - K_2^2) - 2 C_4 K_1 K_2$$

$$C_8 = 2 C_1 K_1 K_2 + C_4 (K_1^2 - K_2^2)$$

Substituting for f and g into the following equations:

$$\sigma x = f g''$$

$$\sigma y = f'' g$$

$$\tau xy = -f'g'$$

gives the following expressions:

$$\sigma x = \frac{E\alpha T_1}{2} (2\ y/b - 1)\ (1 + C_1\ \sinh K_1 x\ \sin K_2 x$$

$$+ C_4\ \cosh K_1 x\ \cos K_2 x)$$

$$\tau xy = - \frac{E\alpha T_1 b}{2} [(y/b)^2 - y/b]\ (C_5\ \sinh K_1 x\ \cos K_2 x$$

$$+ C_6\ \cosh K_1 x\ \sin K_2 x)$$

$$\sigma y = \frac{E\alpha T_1}{2} \frac{b^2}{6} [2\ (y/b)^3 - 3\ (y/b)^2 + 1]\ (C_7\ \sinh K_1 x\ \sin K_2 x$$

$$+ C_8\ \cosh K_1 x\ \cos K_2 x)$$

Heldenfels and Roberts present the solution in a form that is readily adaptable to any dimensions, material, or temperature difference. The accuracy of this approximate solution is estimated to be within ± 5 per cent of the exact solution.

Finite Difference Solution

The second analytical solution to the plane thermal stress equation is a numerical solution. The partial

differential equation is transformed into a finite difference equation by dividing the plate up with a square net, as shown in Figure 2.

For a nodal point O, the equations for the fourth derivatives of ϕ take the following form.

$$\left(\frac{\partial^4\phi}{\partial x^4}\right)_0 \approx \frac{1}{\delta^4}\ (6\phi_0\ -\ 4\phi_1\ -\ 4\phi_3\ +\ \phi_5\ +\ \phi_9)$$

$$\left(\frac{\partial^4\phi}{\partial y^4}\right)_0 \approx \frac{1}{\delta^4}\ (6\phi_0\ -\ 4\phi_2\ -\ 4\phi_4\ +\ \phi_7\ +\ \phi_{11})$$

$$\left(\frac{\partial^4\phi}{\partial x^2\partial y^2}\right)_0 \approx \frac{1}{\delta^4}\ [4\phi_0\ -\ 2(\phi_1\ +\ \phi_2\ +\ \phi_3\ +\ \phi_4)$$

$$+\ \phi_6\ +\ \phi_8\ +\ \phi_{10}\ +\ \phi_{12}]$$

Substituting these equations into the biharmonic equation

$$\frac{\partial^4\phi}{\partial x^4}\ +\ 2\ \frac{\partial^4\phi}{\partial x^2\partial y^2}\ +\ \frac{\partial^4\phi}{\partial y^2}\ =\ -E\alpha\nabla^2T$$

we obtain the finite difference equation for the "O" point.

$$20\phi_0\ -\ 8(\phi_1\ +\ \phi_2\ +\ \phi_3\ +\ \phi_4)\ +\ 2(\phi_6\ +\ \phi_8\ +\ \phi_{10}\ +\ \phi_{12})$$

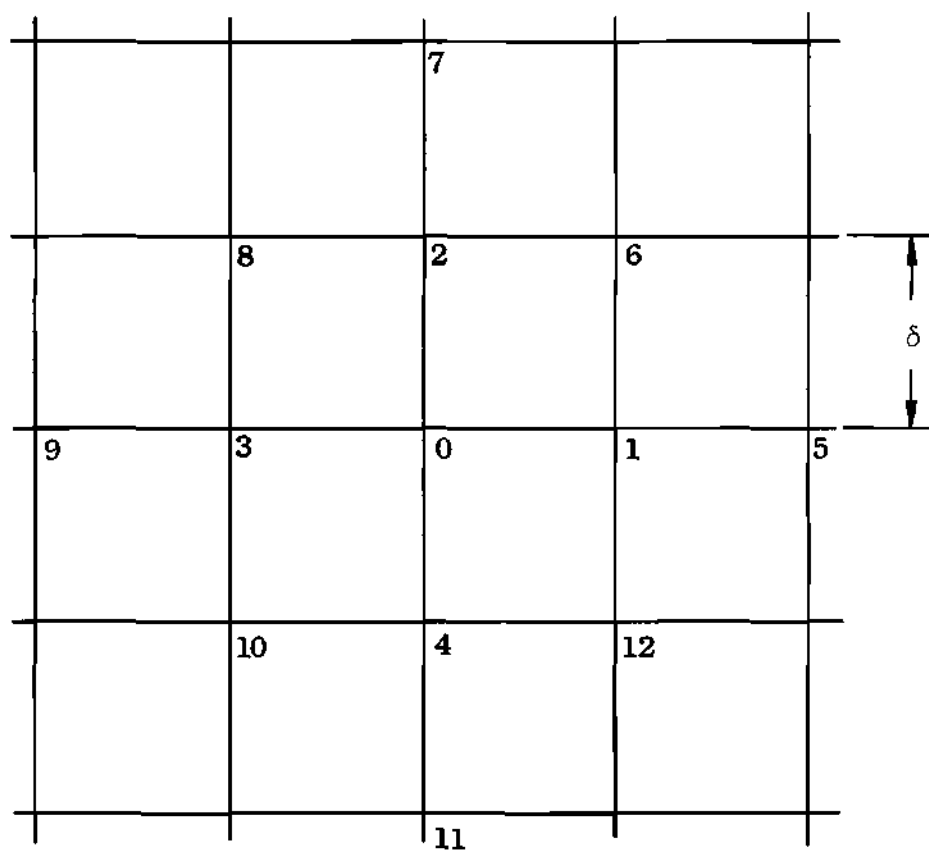$$+\ \phi_5\ +\ \phi_7\ +\ \phi_9\ +\ \phi_{11}\ =\ -\ E\alpha\nabla^2T$$

Figure 2. Grid for Finite Difference Formulation

or in terms of ϕ_0 directly

$$\phi_0 = 0.4(\phi_1 + \phi_2 + \phi_3 + \phi_4) - 0.1(\phi_6 + \phi_8 + \phi_{10} + \phi_{12})$$

$$- 0.05(\phi_5 + \phi_7 + \phi_9 + \phi_{11}) - 0.05 \, E\alpha\nabla^2 T$$

To obtain a solution to this equation, the Laplacian of T must be evaluated. This can be readily solved since the temperature distribution is known and the properties of the material are considered to be constant. The temperature distribution is shown in Figure 3a and the finite difference grid in Figure 3b. The finite difference formulation for the "0" point is:

$$\left(\frac{\partial^2}{\partial x^2} + \frac{\partial^2}{\partial y^2} \right) T \simeq \frac{1}{\delta^2} (T_1 + T_3 - 2T_0) + \frac{1}{\delta^2} (T_2 + T_4 - 2T_0)$$

Since the grid spacing δ is one inch, the expression becomes:

$$\left(\frac{\partial^2}{\partial x^2} + \frac{\partial^2}{\partial y^2} \right) T \simeq (T_1 + T_3 - 2T_0) + (T_2 + T_4 - 2T_0)$$

or

$$\left(\frac{\partial^2}{\partial x^2} + \frac{\partial^2}{\partial y^2} \right) T \simeq (T_1 + T_2 + T_3 + T_4 - 4T_0)$$

T = 150°F

Slope = 10 deg/in.

T = 100°F

T = 50°F

T

X

Y

10 in.

a. Temperature Distribution

T_2

Y

Horizontal
Centerline

T_3 T_0 T_1

X

$\delta = 1$ in.

T_4
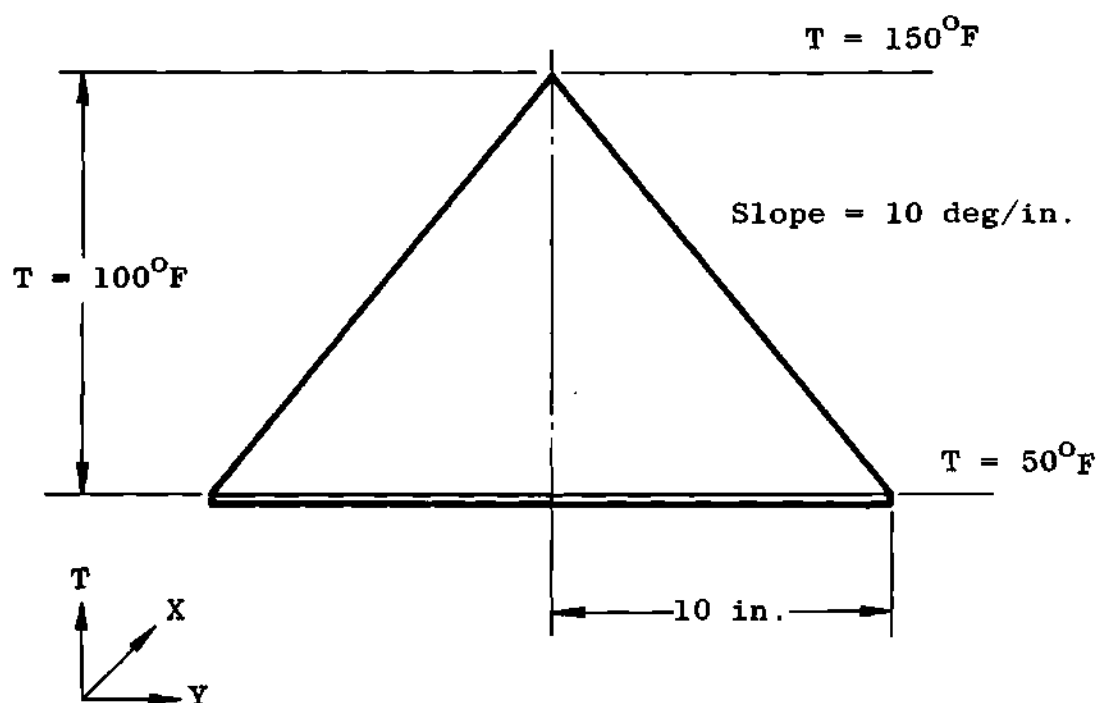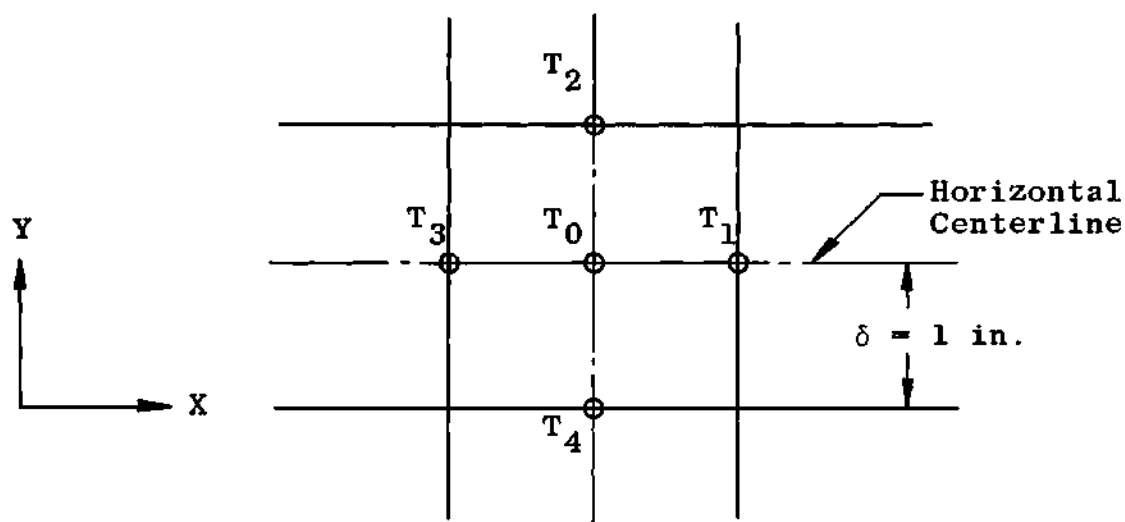
b. Laplacian Finite-Difference Grid

Figure 3. Temperature Profile and Finite-Difference
Grid for the Rectangular Plate

Substituting temperatures from Figure 3a:

$$\left(\frac{\partial^2}{\partial x^2} + \frac{\partial^2}{\partial y^2}\right) T \simeq (100 + 90 + 100 + 90 - 400) = -20$$

This value of the Laplacian is valid for the heated center-line only and can be shown to be zero elsewhere.

Substituting into the finite difference equation for ϕ_0 gives

$$\phi_0 = 0.4(\phi_1 + \phi_2 + \phi_3 + \phi_4) - 0.1(\phi_6 + \phi_8 + \phi_{10} + \phi_{12})$$

$$-0.05(\phi_5 + \phi_7 + \phi_9 + \phi_{11}) + 0.05(20E\alpha)$$

or for any nodal point in the plate grid

$$\phi_{i,j} = 0.4(\phi_{i,j+1} + \phi_{i,j-1} + \phi_{i+1,j} + \phi_{i-1,j})$$

$$-0.1(\phi_{i+1,j+1} + \phi_{i+1,j-1} + \phi_{i-1,j+1} + \phi_{i-1,j-1})$$

$$-0.05(\phi_{i,j+2} + \phi_{i,j-2} + \phi_{i+2,j} + \phi_{i-2,j})$$

$$+0.05 \ (20E\alpha)$$

where $i,j = 1, 2, 3, \ldots, n$.

This equation must be satisfied at every nodal point of the grid within the boundary of the plate.

The boundary conditions are

$$\phi_{i,j} = 0 \qquad \text{for } i = 0,\ A/2$$

$$\phi_{i+1,j} = \phi_{i-1,j} \qquad j = 1,\ 2,\ \ldots,\ (A/2 - 1)$$

$$\phi_{i,j} = 0 \qquad \text{for } i = 1,\ 2,\ \ldots,\ (A/2 - 1)$$

$$\phi_{i,j+1} = \phi_{i,j-1} \qquad j = 0,\ A/2$$

The boundary conditions $\phi_{i+1,j} = \phi_{i-1,j}$ and $\phi_{i,j+1} = \phi_{i,j-1}$ represent the zero normal slope condition where imaginary grid points have been established outside the boundary.

CHAPTER IV

THE ANALYTICAL PROGRAM

The analytical program considered the solutions to a plate, as shown in Figure 1, with the following physical properties:

$$A - 30 \text{ inches}$$

$$B - 20 \text{ inches}$$

$$b - 1 \text{ inch}$$

$$t - 0.25 \text{ inch}$$

$$\alpha - 6.5 \times 10^{-6}/{}^{\circ}F$$

$$E - 30 \times 10^{6} \text{ psi}$$

$$\Delta T - 100^{\circ}F$$

The solution of Heldenfels and Roberts and the finite difference solution were programmed for the solution of the above problem on the Burroughs 220 Electronic Computer using the Burroughs Algebraic Compiler.

In the solution by Heldenfels and Roberts, one-quarter of the plate was used because of the symmetry about the longitudinal and transverse centerlines. This quarter of the plate was covered with a one-inch by one-inch grid network. Solutions were obtained at all the grid intersections or nodal points on the face of the plate, which for this configuration was 176. The nodal solutions were printed out in

values for x, y, σx, σy and τxy. Some difficulty was experienced initially in getting the program to run satisfactorily. This was remedied by manually calculating the values of C_1 and C_4 and using these values as inputs in the program. This program was also run for a ΔT of $50^{\circ}F$ for comparison purposes as the stress values are a direct function of ΔT and should vary proportionally. The results of the $\Delta T = 100^{\circ}F$ program are shown in Figures 4 through 9.

The finite difference solution had to be evaluated numerically. There is a linear equation for ϕ at each of the interior nodal points which also involves the value of ϕ at the twelve surrounding nodal points. The equations for points adjacent to the boundaries reflect the boundary conditions imposed upon them. There are two commonly used methods for solving a system of equations of this type. They both involve an iteration process after making an initial guess as to the answer. The accuracy of the guess is reflected in the size of the residual or remainder after the calculation has been carried out. The closer the initial guess, the smaller the residual. If the exact solution were guessed, the equation would be satisfied and the residual would be zero.

These two methods of numerical solution are known as the Southwell Relaxation[3] and the Gauss-Seidel[4]. In the Southwell method, the point with the largest residual is selected and reduced to zero by adjusting ϕ. The next largest residual is then reduced and this continues until all points
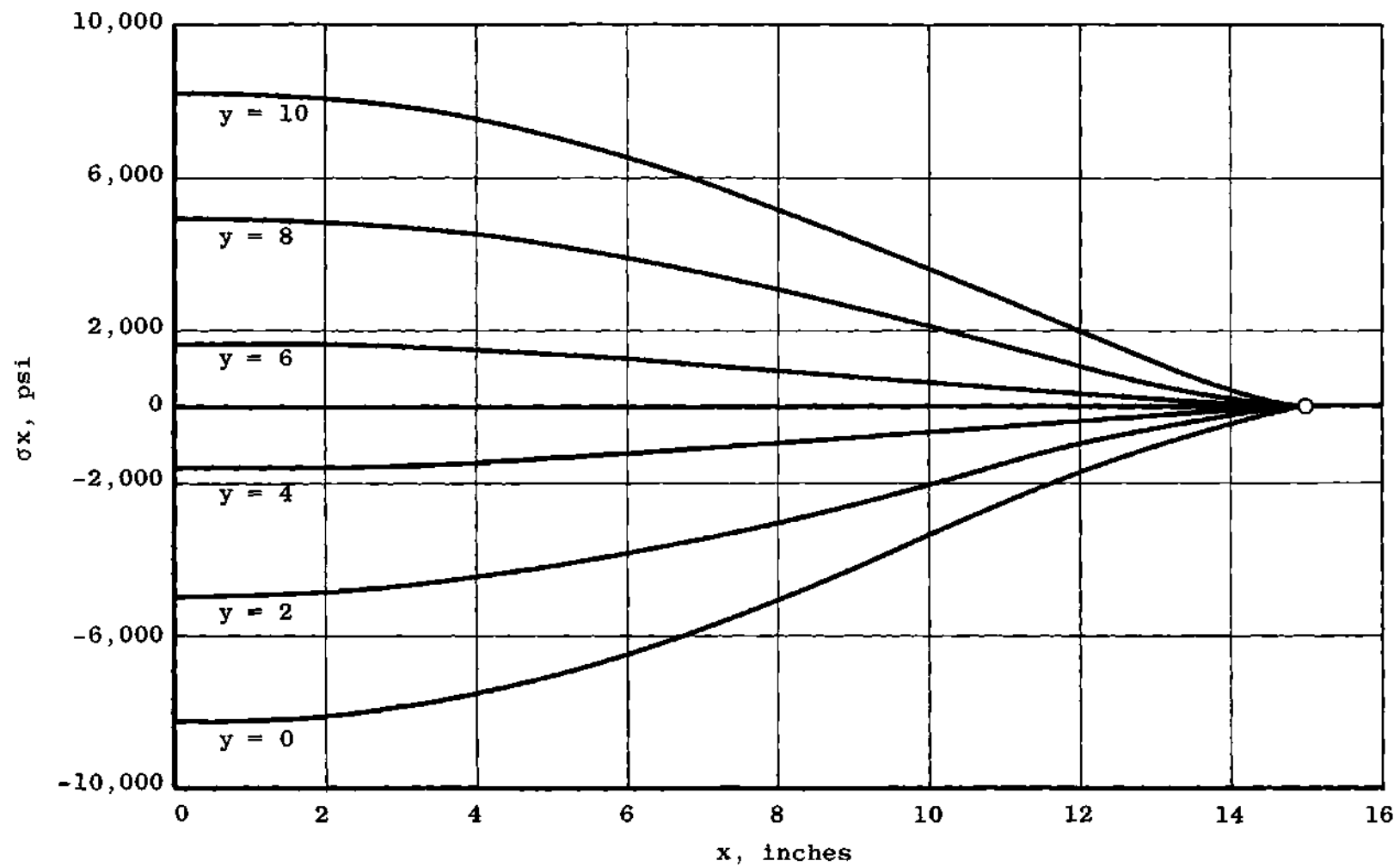
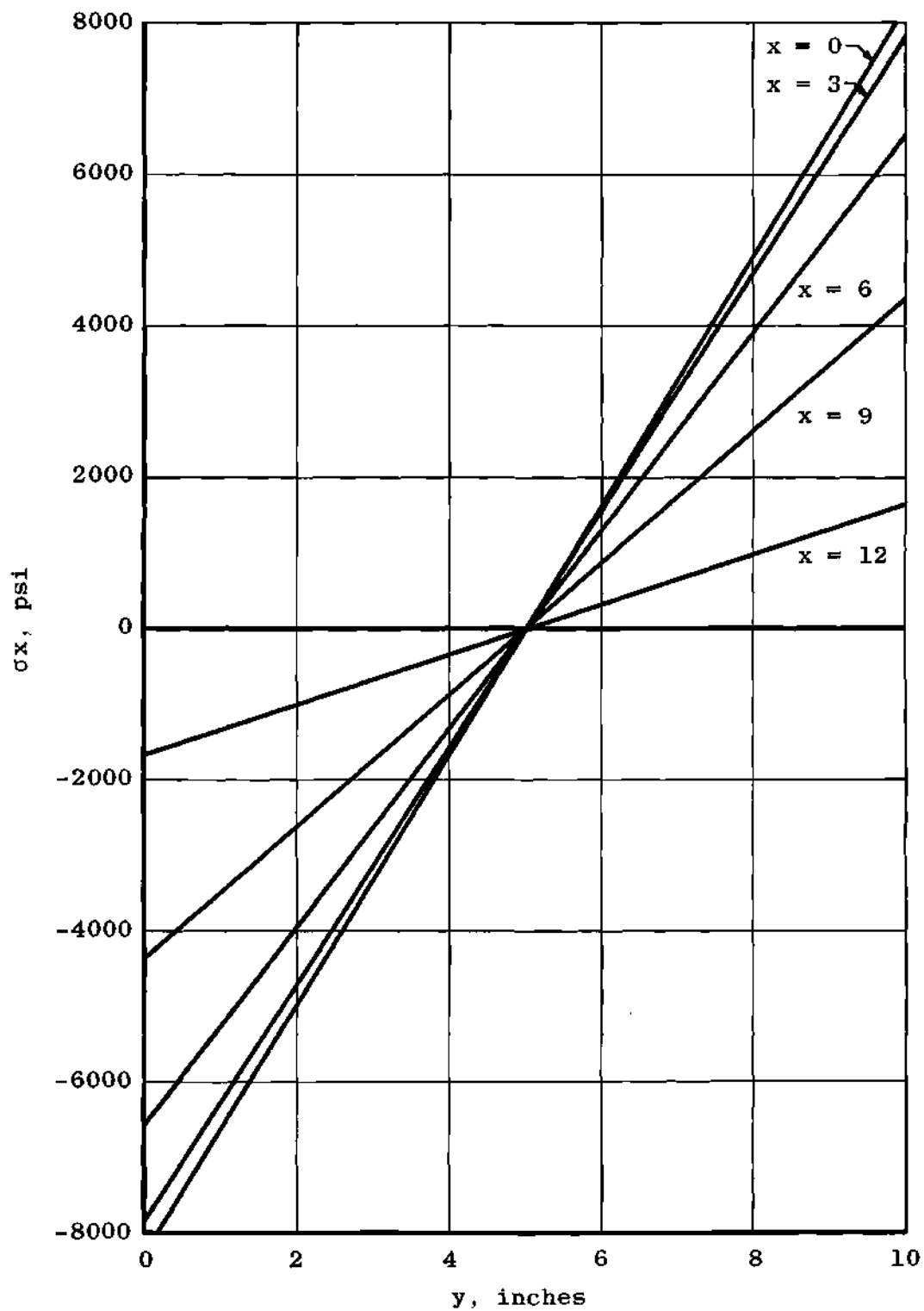Figure 4. Heldenfels and Roberts Solution,
Longitudinal σx

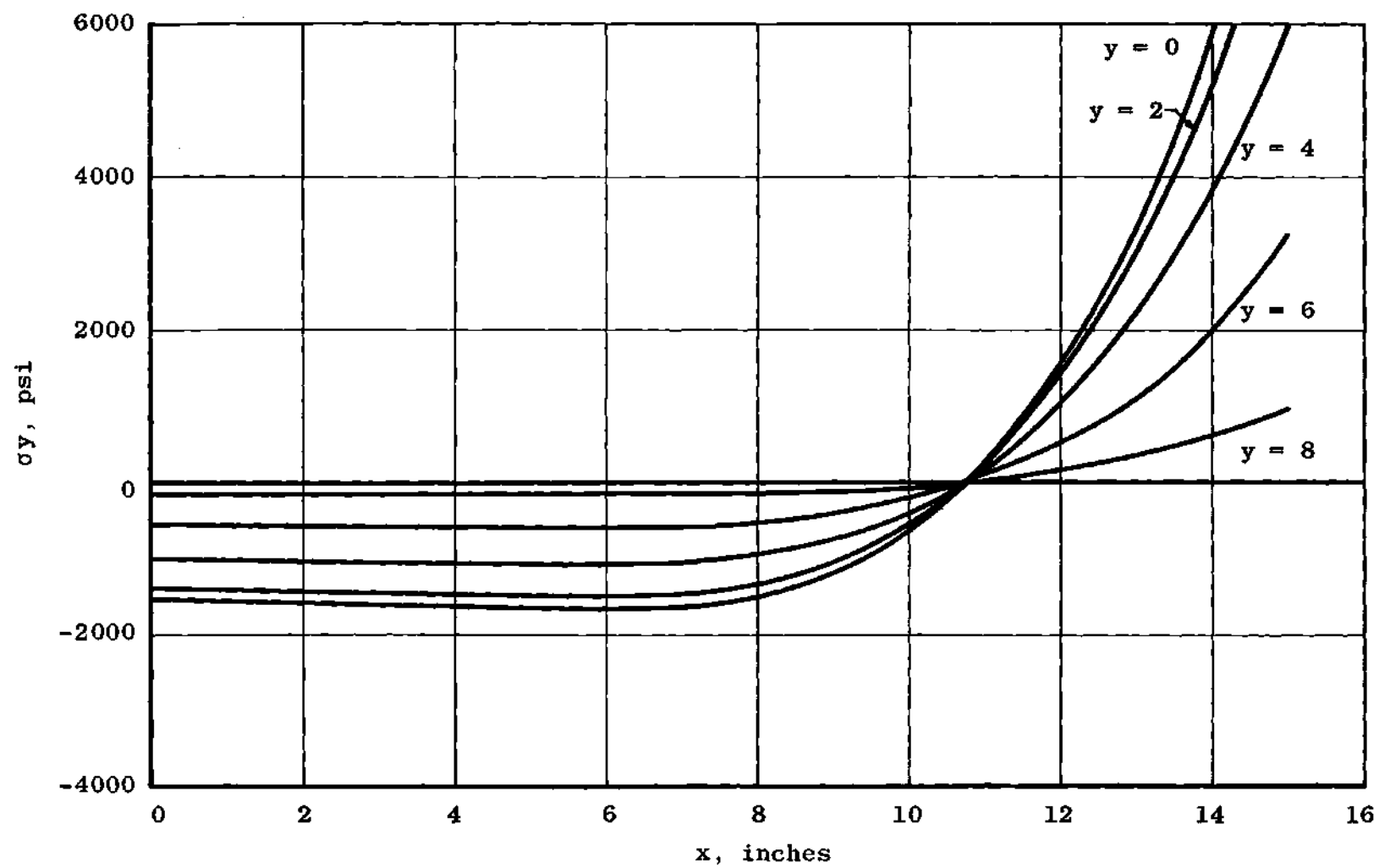Figure 5. Heldenfels and Roberts Solution,
Transverse σx

Figure 6.   Heldenfels and Roberts Solution,
Longitudinal σy

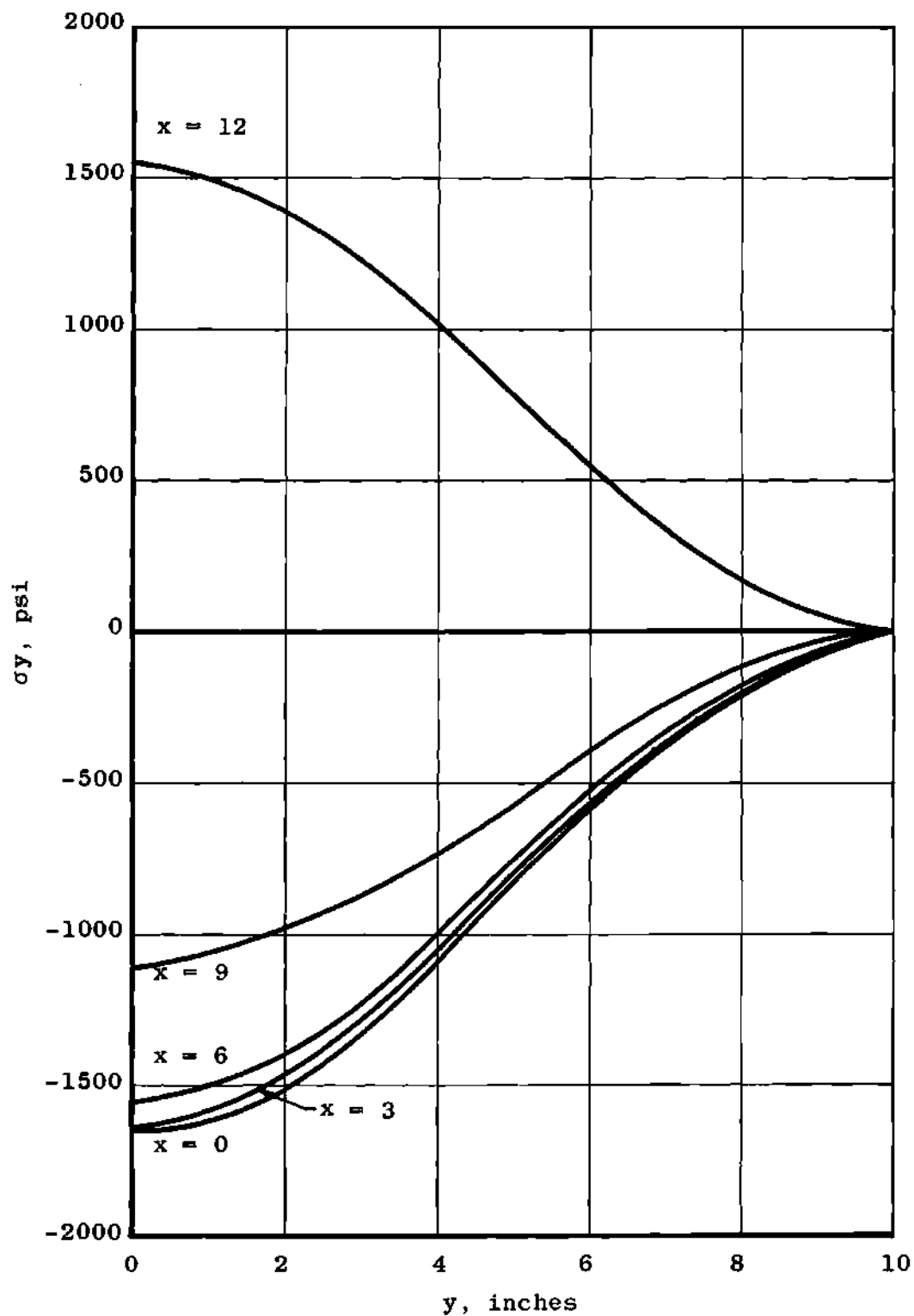Figure 7.   Heldenfels and Roberts Solution,
Transverse σy

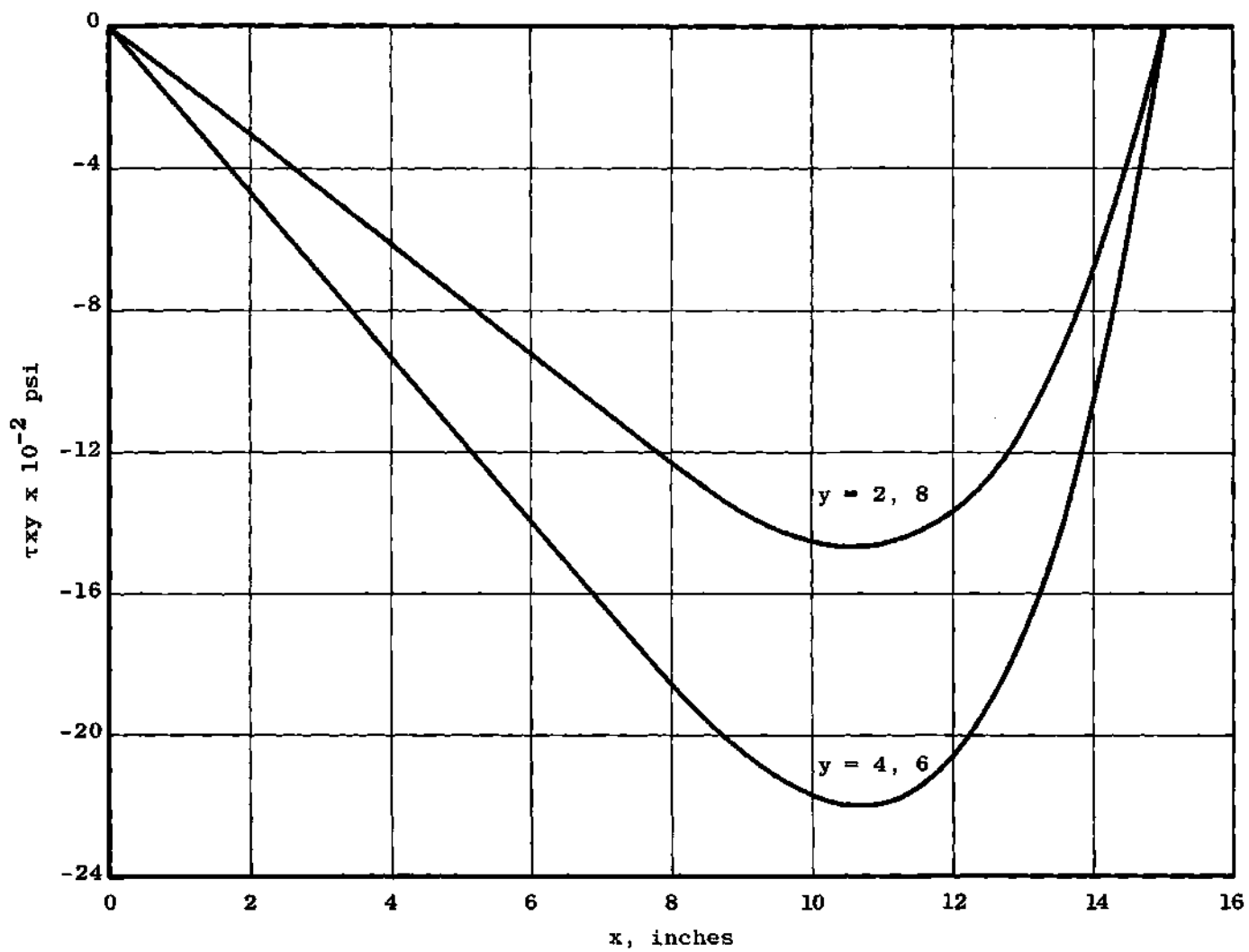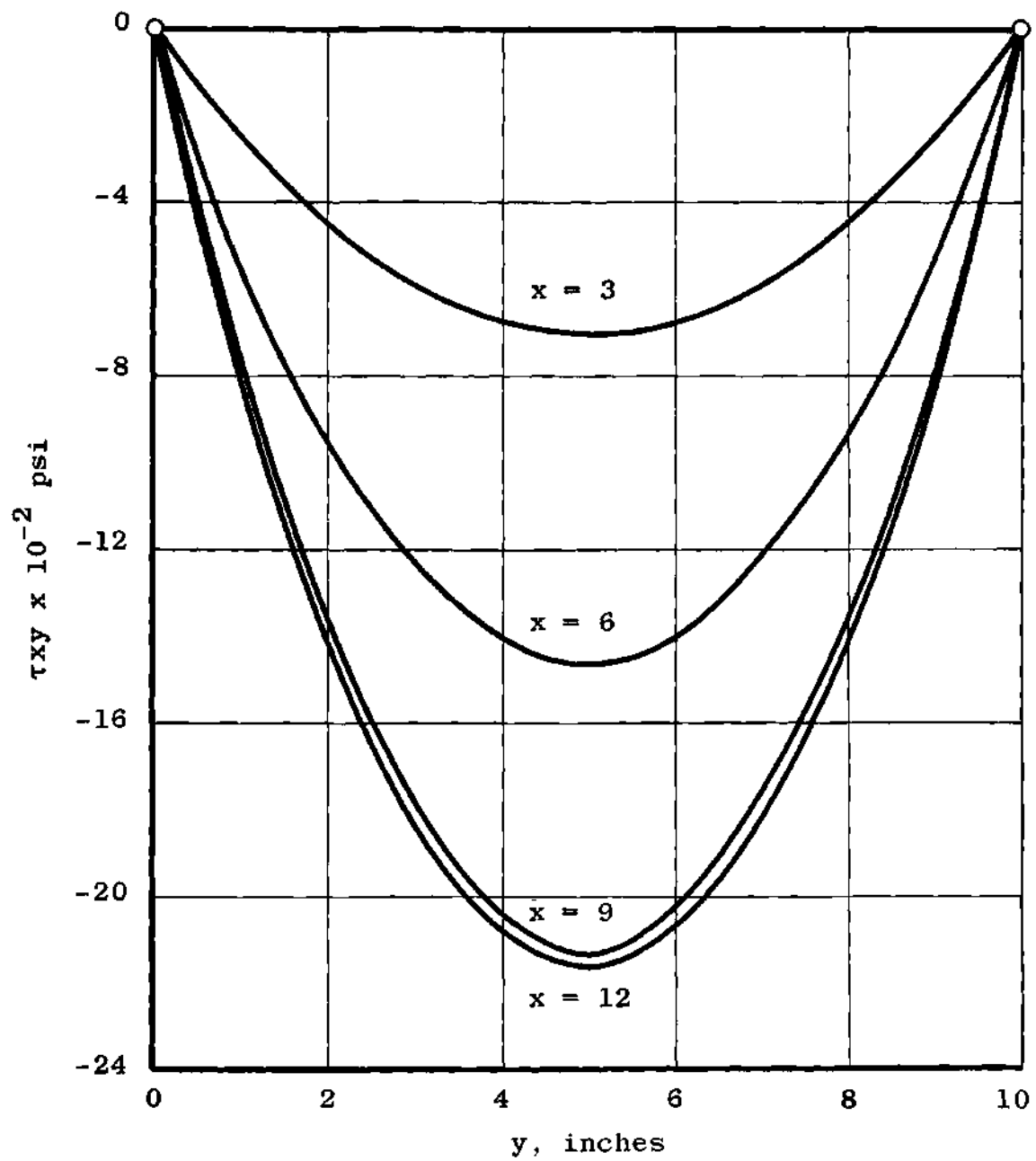Figure 8.   Heldenfels and Roberts Solution,
Longitudinal τxy

Figure 9. Heldenfels and Roberts Solution,
Transverse τxy

have been reduced. The entire process is then repeated and continued until the residuals of all points are reduced to an acceptable value. The Gauss-Seidel method does not differentiate between the size of the residuals, but steps from point-to-point, reducing each residual in turn. This process also repeats itself until the residuals are sufficiently low. The Gauss-Seidel method was used in this program because it was felt that the total computer time would be less if the computer did not have to examine a row of residuals and make a selection before it did the relaxation.

One-quarter of the plate was again used because of longitudinal and transverse symmetry. The quarter used was covered with a grid network of one-inch squares. The additional grids were required because of the imaginary points located outside of the boundary which were needed to solve for ϕ at the edge of the plate. The initial guess of the values of ϕ was zero everywhere. The computer then started reducing the residuals from the input information. The calculation of the stresses by this method was found to be extremely slow. The time required for 10,000 iterations was 30 minutes, and the resulting stress values gave good correlation with the values calculated by the Heldenfels and Roberts solution. If unlimited computer time were available, the finite difference equations could be satisfied by running the program for several thousand more iterations to obtain a very good approximation to the actual stress values. For any

reasonable expenditure of computer time, however, the approximation to the actual stress values is rather poor. For this type of problem, the method of numerical relaxation used by Murphy[5] is far superior to either the Gauss-Seidel or Southwell Relaxation Methods.

In this particular problem, the numerical value of the Laplacian was 195, within the limits $9.5 < y < 10.5$, for the 100^OF temperature gradient. The answers obtained for each nodal point (i, j) were $\phi_{i,j}$, $\sigma x_{i,j}$, $\sigma y_{i,j}$, and $\tau xy_{i,j}$. In Figures 10 through 15, for a ΔT of 100^OF, the results of the several iterative calculations are shown plotted with the Heldenfels and Roberts Solution.
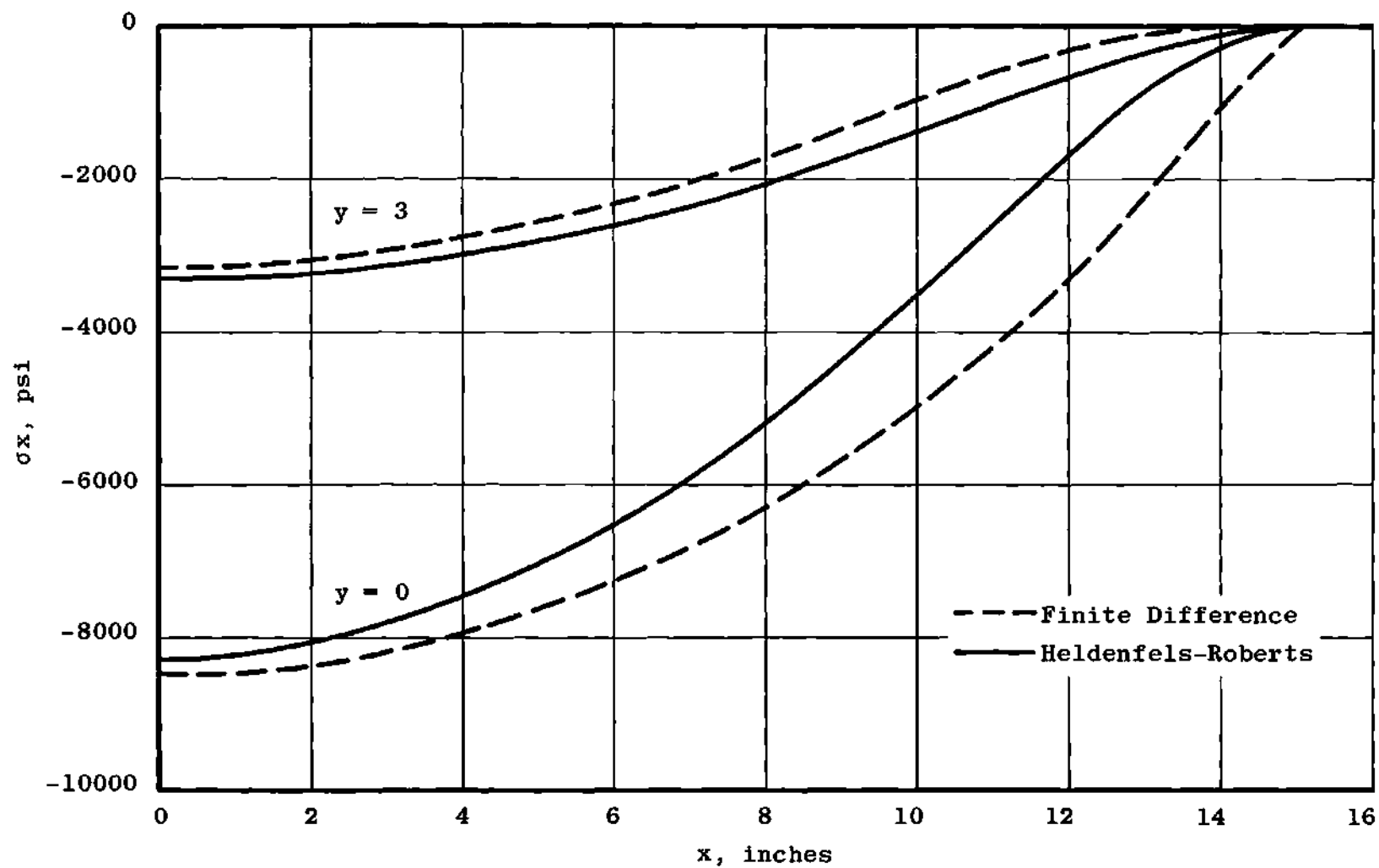
Figure 10. Finite Difference Solution,
Longitudinal σx
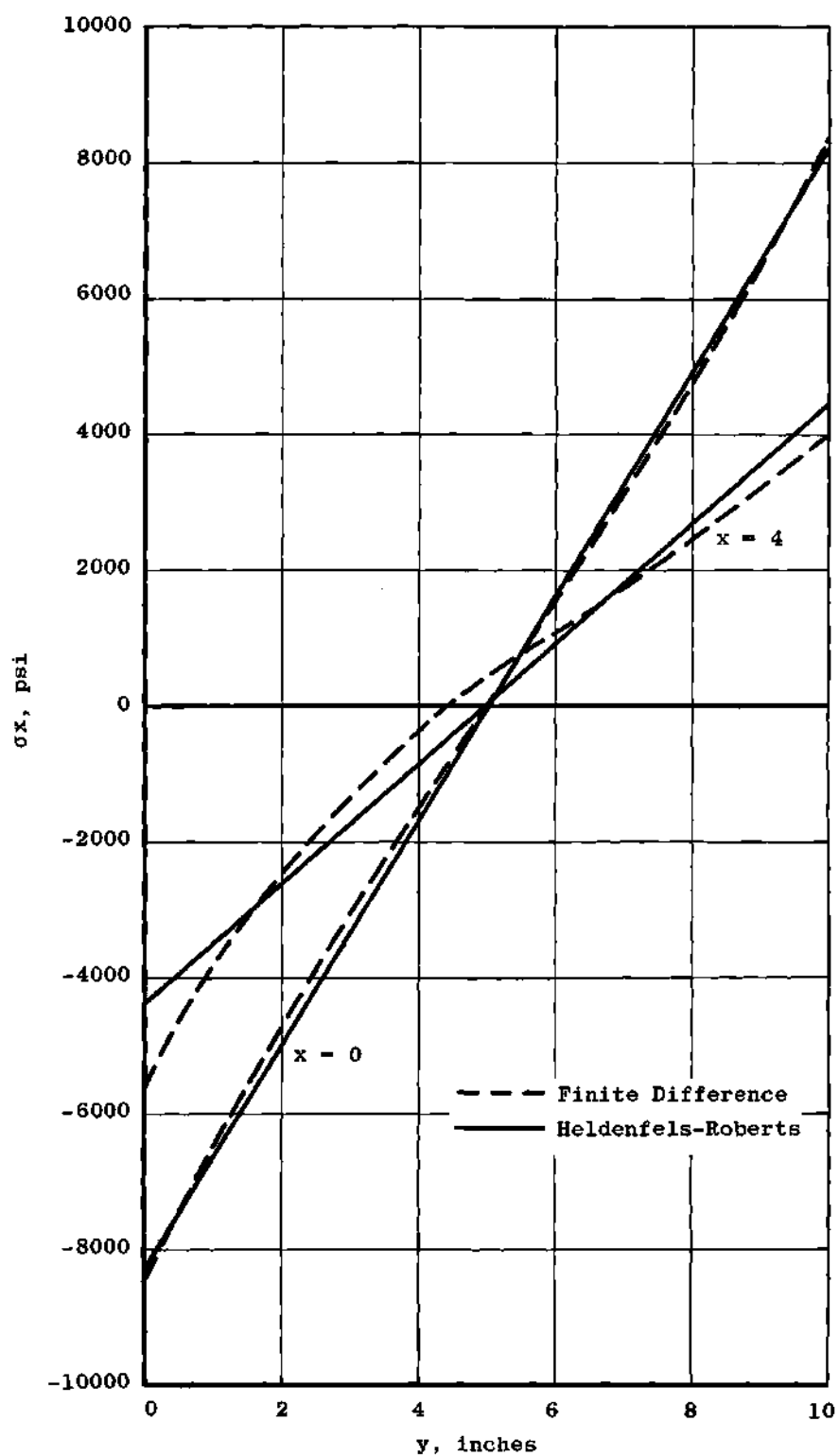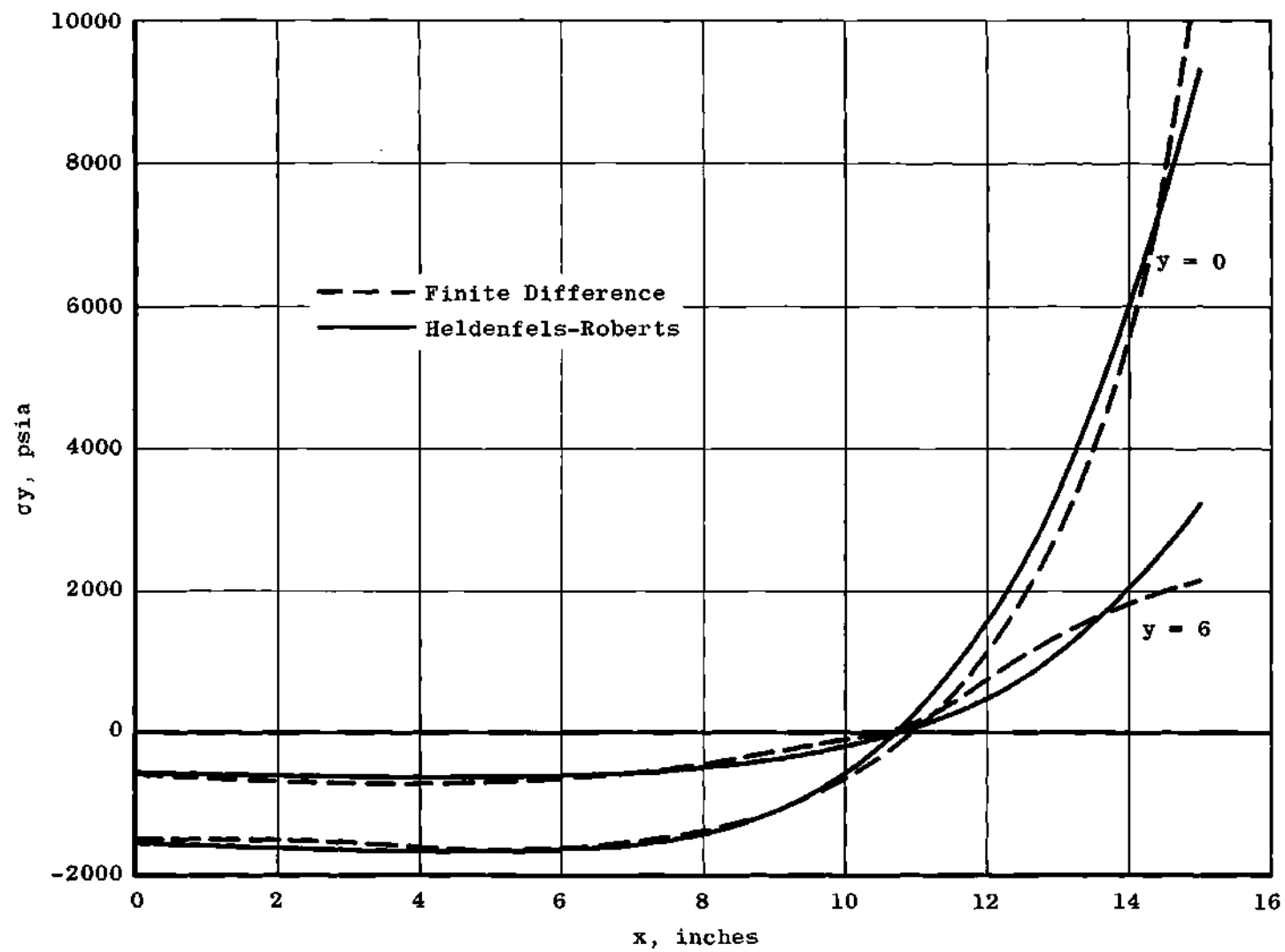
Figure 11. Finite Difference Solution,
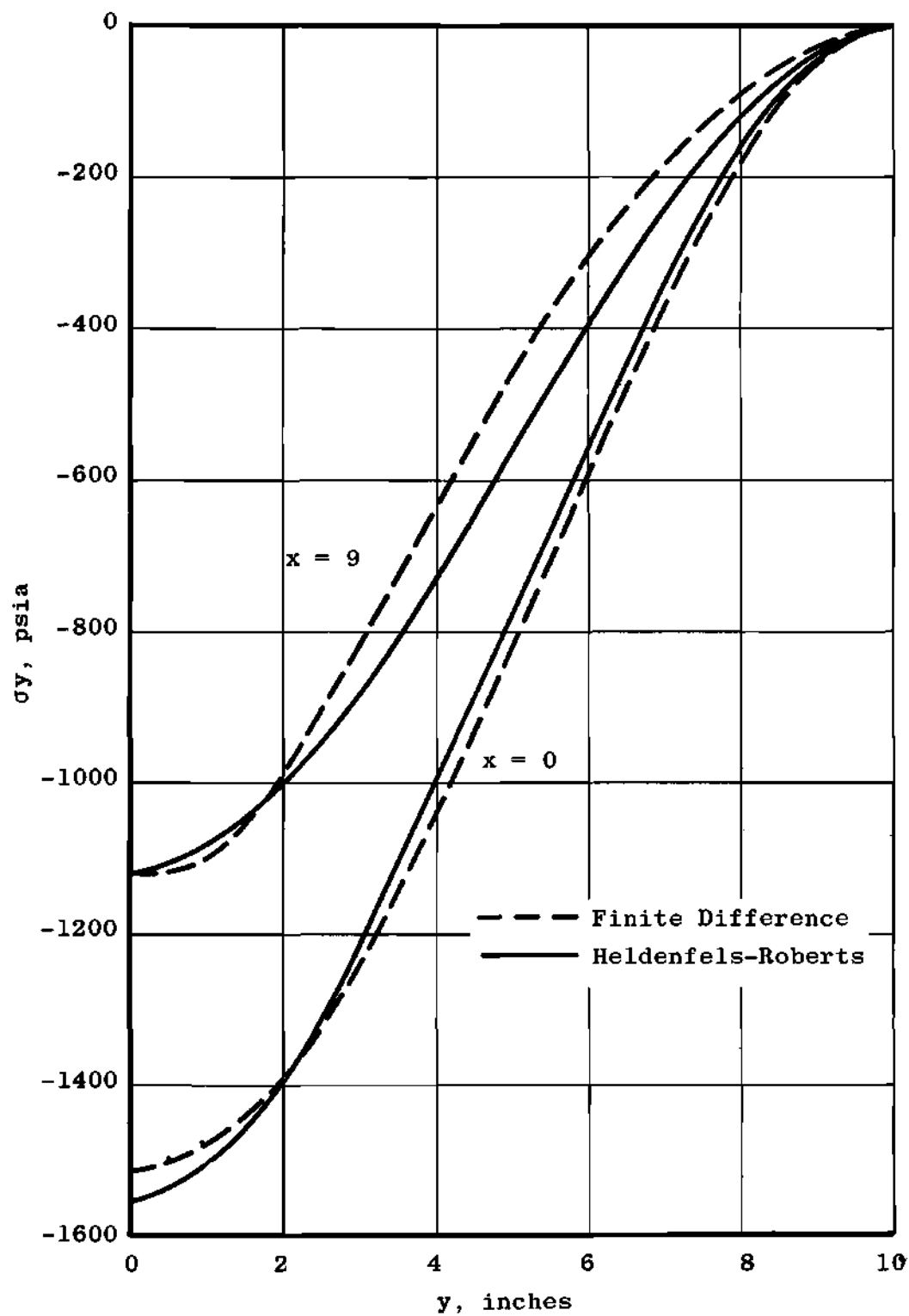Transverse σx

Figure 12. Finite Difference Solution,
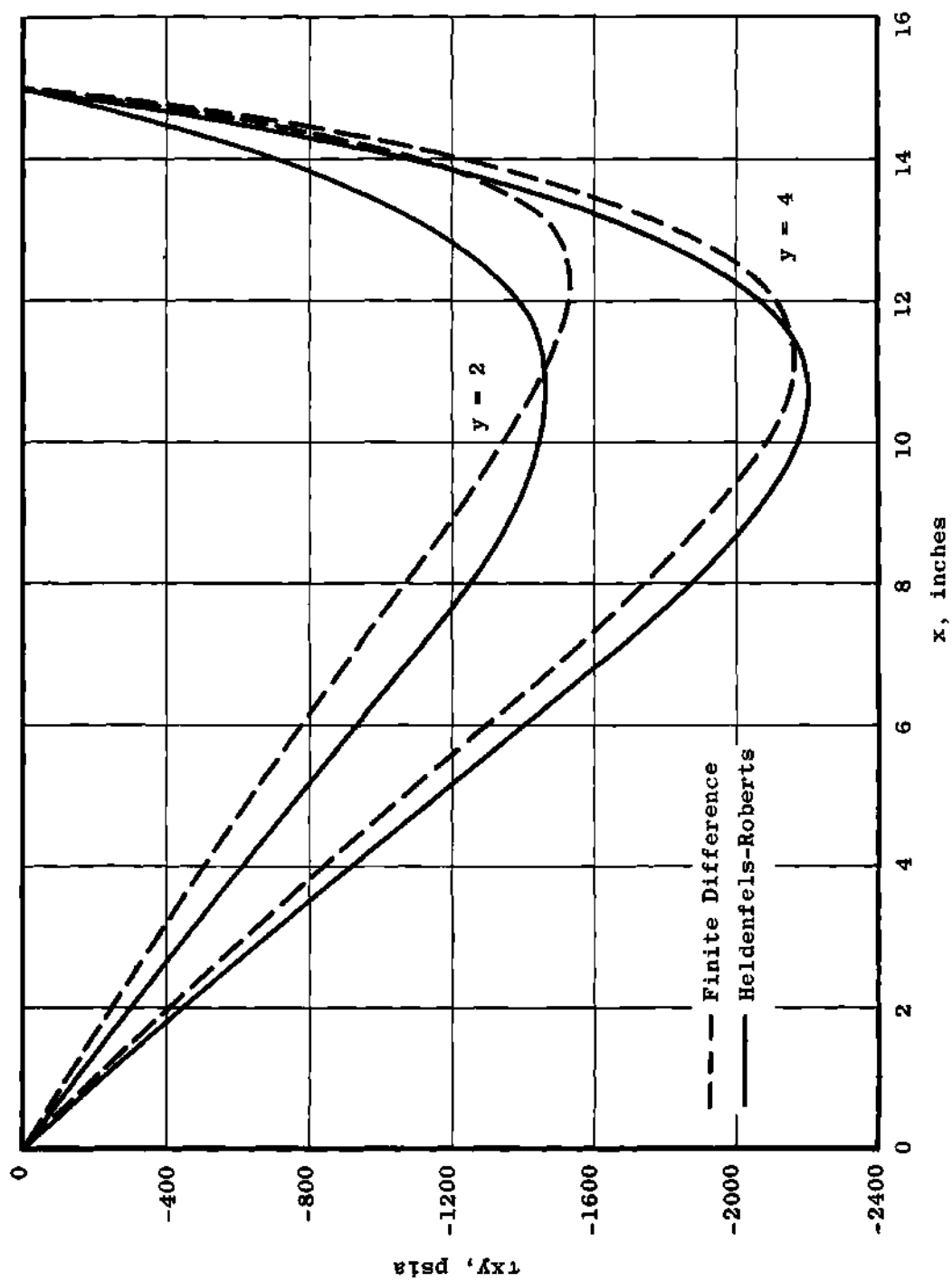Longitudinal σy

Figure 13.   Finite Difference Solution,
Transverse σy
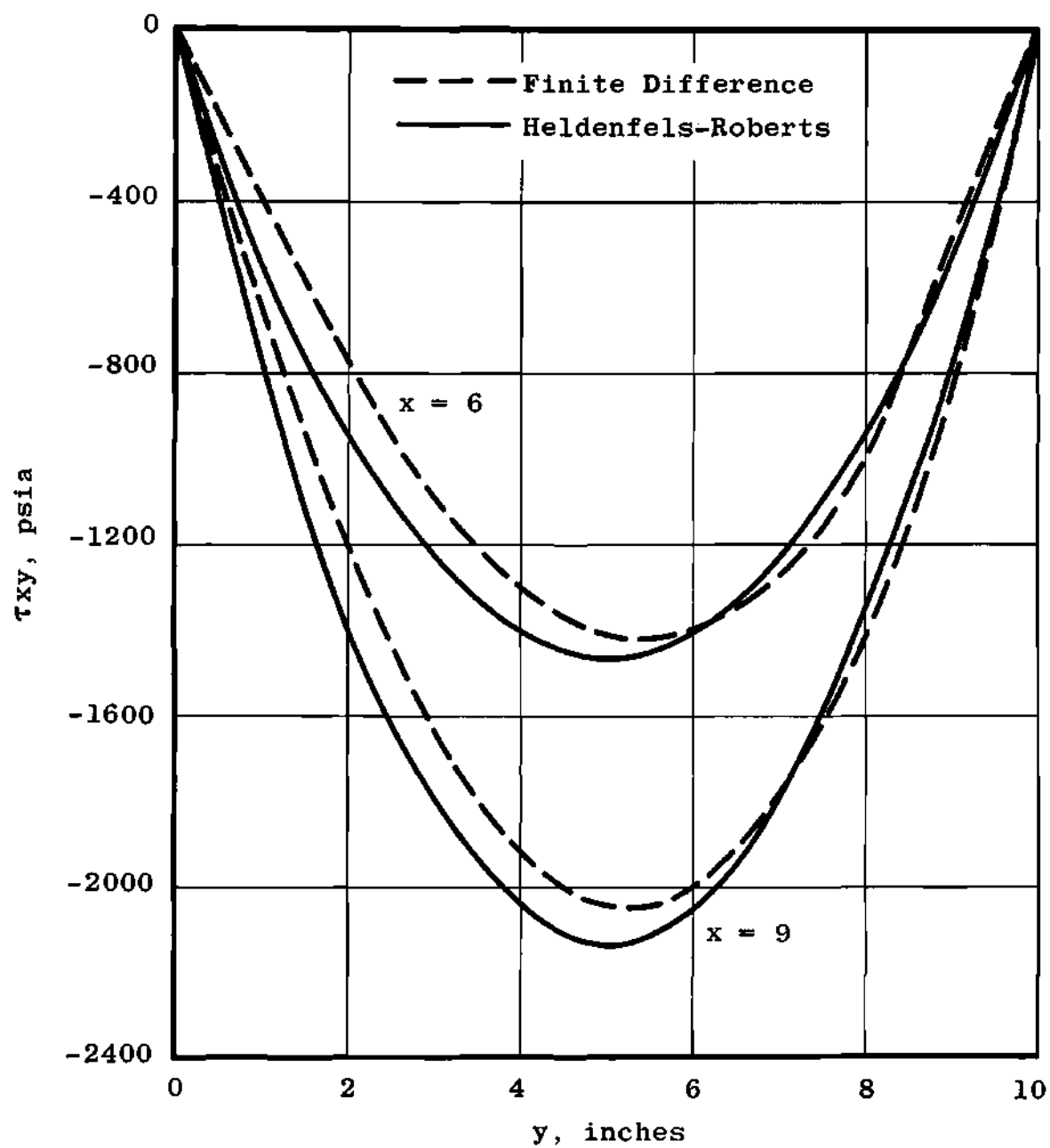
Figure 14. Finite Difference Solution,
Longitudinal τxy

Figure 15. Finite Difference Solution,
Transverse τxy

CHAPTER V

THE EXPERIMENTAL PROGRAM

The experimental program was conducted so that the
results could be compared with the analytical approximate
solutions. A mild steel plate (0.18 to 0.20 percent carbon)
was the subject of the investigation. The plate was 20-inches
by 30-inches by 0.25-inch thick and had the same properties
used in the analytical programs. The plate was hot rolled,
and the direction of rolling coincided with the larger dimen-
sion. It was obtained in a 24-inch by 36-inch size and was
machined to the test size. The excess material from the
trimming and machining was used to fabricate tensile test
specimens. Specimens were cut both in the longitudinal and
the transverse directions of rolling for determining the
relative tensile properties. The test plate and the tensile
test specimens were annealed for two hours at 600^OF in an
electric oven to relieve any residual stress from the rolling
operation. After the annealing, tensile tests were run on
the specimens. The results of these tests showed that the
tensile strength of the transverse specimens was about
five per cent greater than the longitudinal specimens. It
was decided to use the data from the longitudinal tests be-
cause the predominant stresses lie in the longitudinal

direction. The stress-strain curve shown in Figure 16 was drawn from these data.

The heat input to the plate was supplied by two G. E. calrod heaters, catalog number 5-D-12. The heaters were sandwiched between two one-inch-wide by one-half-inch-thick copper bars which were machined out to admit them. The bars were then mechanically fastened together. The heaters required 200 watts of power each at 110-volts ac and were connected in parallel to the temperature-control Variacs.

The temperature profile across the plate was maintained by cooling the longitudinal edges. This was accomplished by running cooling water through two 0.25-inch, thick-walled copper pipes. The pipes were machined flat on one side to fit the plate edge smoothly. A small lip was left at one edge of the flat surface to assist in the vertical alignment of the pipe and plate. The pipe inlets were connected to a common manifold with individual valves so that the flow rate through each pipe could be separately controlled. The cooling water was supplied from the city mains at prevailing temperature. Neither pressure nor temperature of the water were measured as the cooling capabilities were always adequate to establish the desired thermal gradient.

The thermal gradient was monitored with 20 iron-constantan thermocouples arranged over the surface of the plate. The location of the thermocouples is shown in Figure 17. The locations were selected to provide a check
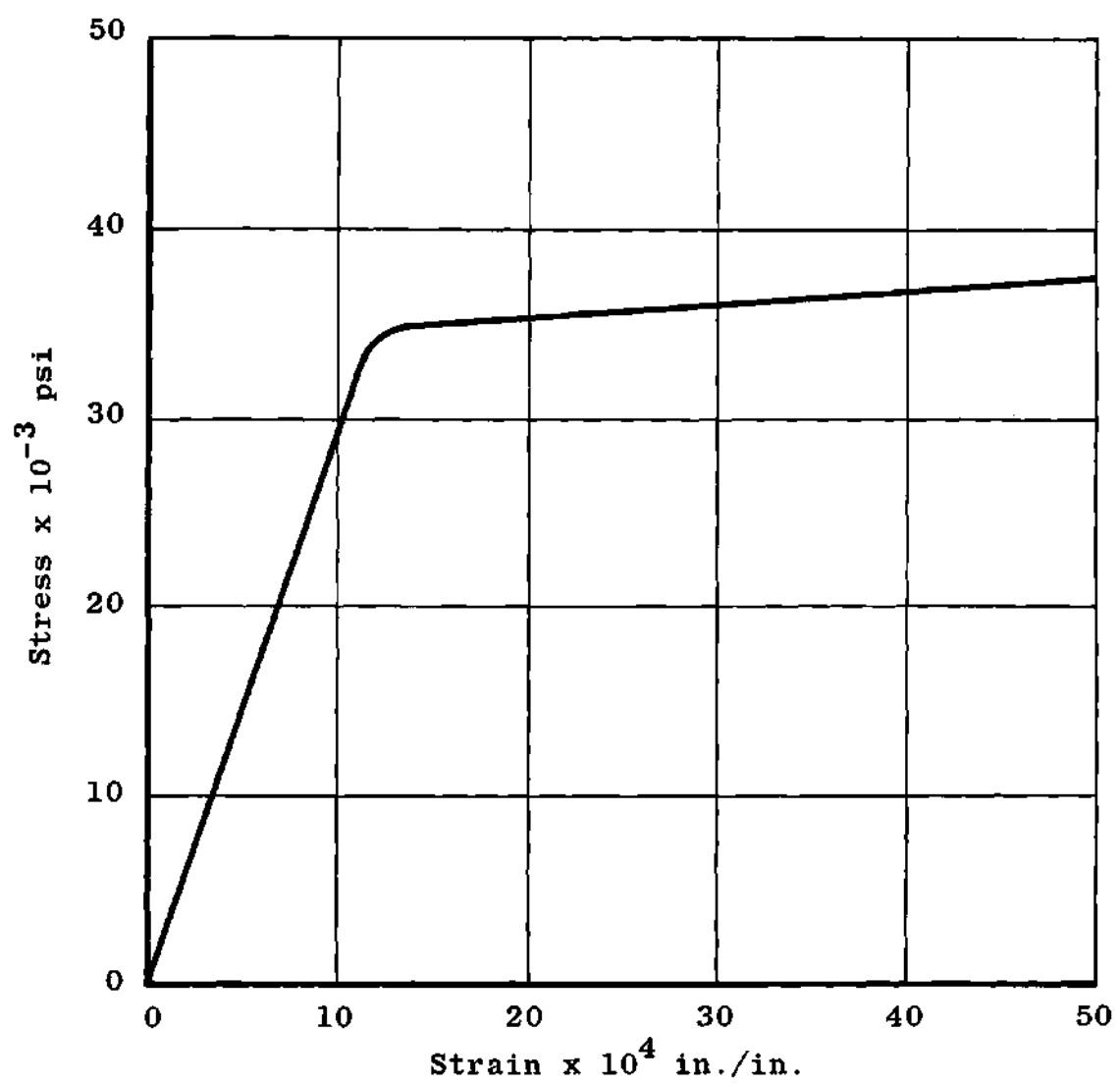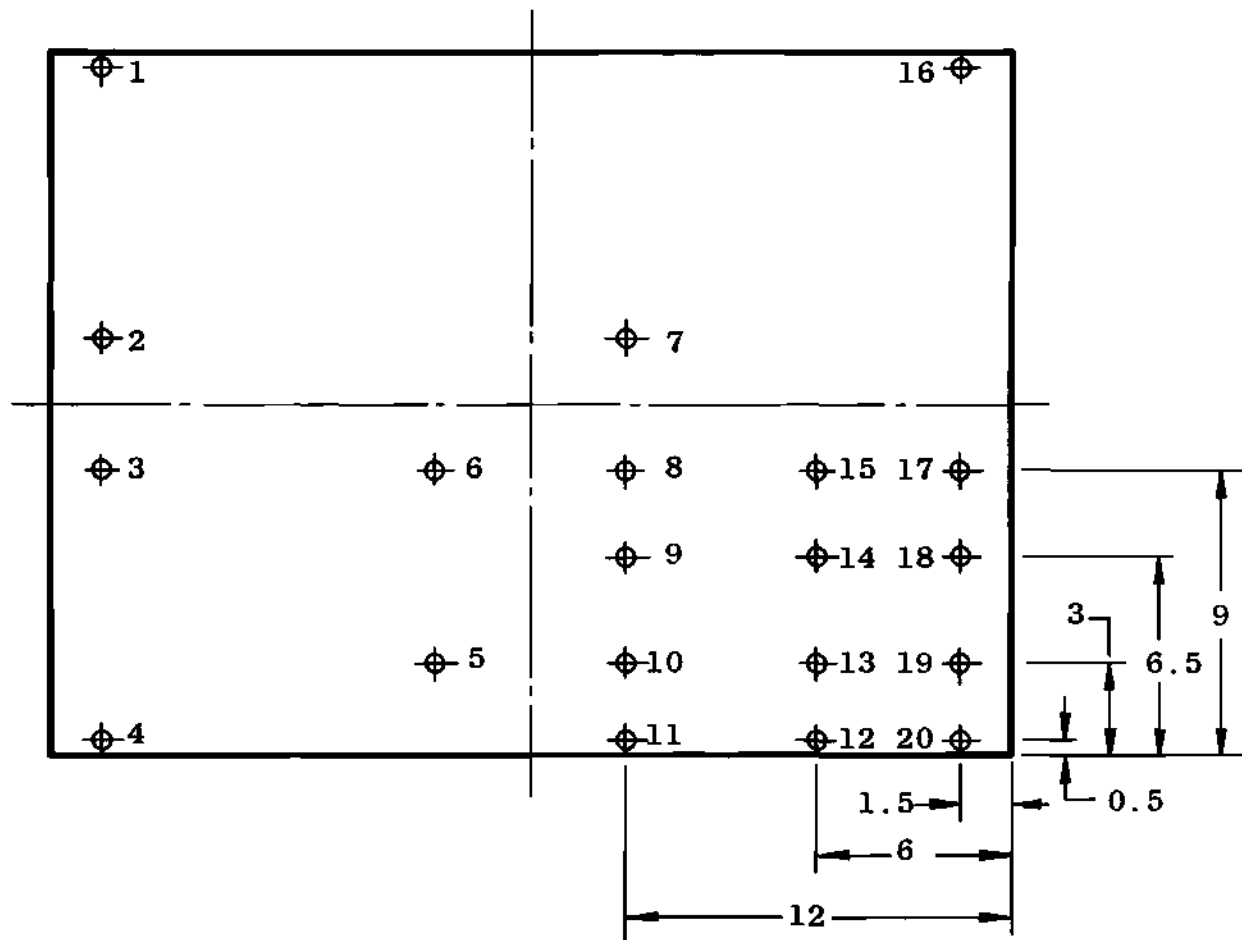
Figure 16. Stress-Strain Curve for Rectangular Plate Material

Dimensions are in inches.

Figure 17. Thermocouple Location on the Rectangular Plate

of the gradient or profile in the transverse and longitudinal directions and to determine the plate temperature at the strain gage locations. The thermocouples were fabricated by butt-welding a junction in 24-gage, iron-constantan thermocouple wire with glass-on-glass insulation. The wire was manufactured by the Thermoelectric Corporation. The thermocouples were installed in the plate by drilling small indentations approximately 3/32-inch diameter by 1/64-inch deep, inserting the thermocouple junctions, and securing them in close physical contact with Sauereisen Type 63, electric heater cement. The thermocouple leads were brought out to an enclosed, isothermal, terminal strip and then into a switching circuit for readout. The temperatures were read on a Leeds and Northrup Type No. 8962, self-compensated, portable temperature potentiometer.

The temperature of the plate was controlled by a Leeds and Northrup Series 60 controller used in conjunction with a Leeds and Northrup Speedomax G Recorder. Thermocouples 7 and 8 were connected in parallel and used as the control input to the recorder. The desired temperature of the plate centerline was determined in millivolts output for the iron-constantan thermocouple and was manually set in the recorder as the control point. The output of the controller Variac was used as the input to a manually controlled Variac connected to the heaters. The second Variac was used to reduce the heat input and allow uniform temperature increases

through the plate. The temperature controller proved to be an invaluable piece of equipment, and the experimental phase could hardly have been accomplished without it. It was capable of establishing and maintaining any desired temperature within $\pm 0.5^{\circ}$F. If it had been necessary to establish the desired temperature profile under steady-state conditions manually, the experimental phase of the work would have taken an unreasonable length of time.

The basic data from the experimental program were the strain measurements made with bonded strain gages. The strain gage used in this investigation was the Baldwin SR-4 Temperature-Compensated Strain Gage, Type EBF-7S+[6]. This gage was selected as a result of investigations made on the subject by Murphy. The EBF-7S+ provides reasonably good temperature compensation to about 250°F when mounted on structural type (1020) steel. The grid of this gage is made up of two constantan elements, one with a negative coefficient and the other with a positive coefficient combined in the correct resistance ratio to correct for thermal expansion of a specific material. The advantage of this gage over the conventional gage is that it eliminates the necessity of maintaining a dummy gage at the same temperature as the measuring gage. Data included with the gage gave its resistance as 120 ± 0.5 ohms and gage factor as 2.04 ± 1 per cent. Figure 18 shows a drawing of the gage.
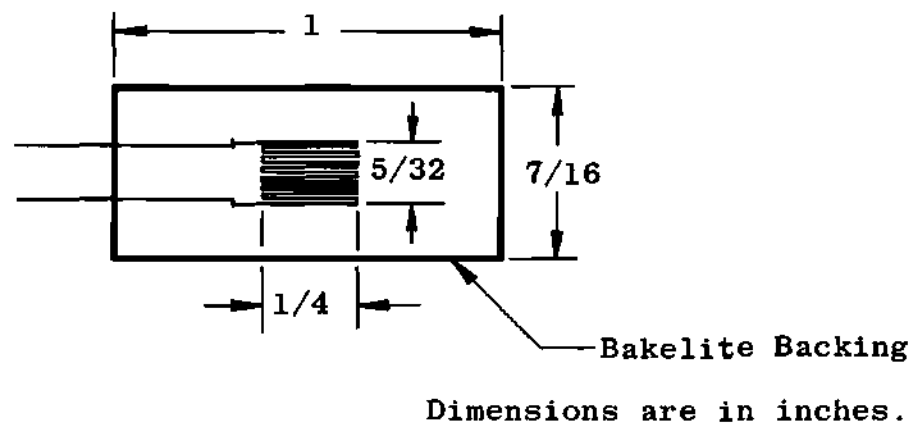
Figure 18. Dimensioned Sketch of the EBF-7S+ Strain Gage

The eight strain gages were all located on the transverse centerline. Five of the gages were oriented to measure longitudinal strain and three to measure transverse strain, as shown in Figure 19.

Mounting of the gages to the plate proved to be a tedious task. The plate had to be cleaned of all scale in the immediate area of gage application and a suitable finish obtained on it. The bonding agent was a bakelite cement recommended by Baldwin-Lima-Hamilton for use with this type of gage. After the gages were applied to the plate, they had to be subjected to a pressure of 100 psi and put through a six-hour curing cycle. The curing cycle brought the gage cement up to the polymerizing temperature slowly to allow the solvents to be driven off without creating voids by bubbling. At the end of the cycle, the pressure was removed from the gages, and then the plate and gages were cycled several times from ambient temperature to a temperature greater than would be encountered in the test. The cycling is necessary to stabilize the cement which bonds the gages, and reproducible strain readings cannot be obtained without it.

After the installation and wiring of the gages, a nichrome strip was spot-welded to the gage leads and to the connecting wires. The wires were 26-gage, "tinned" copper with Fiberglas insulation. To prevent damage to the strain-gage leads, the connecting wires were cemented to the plate
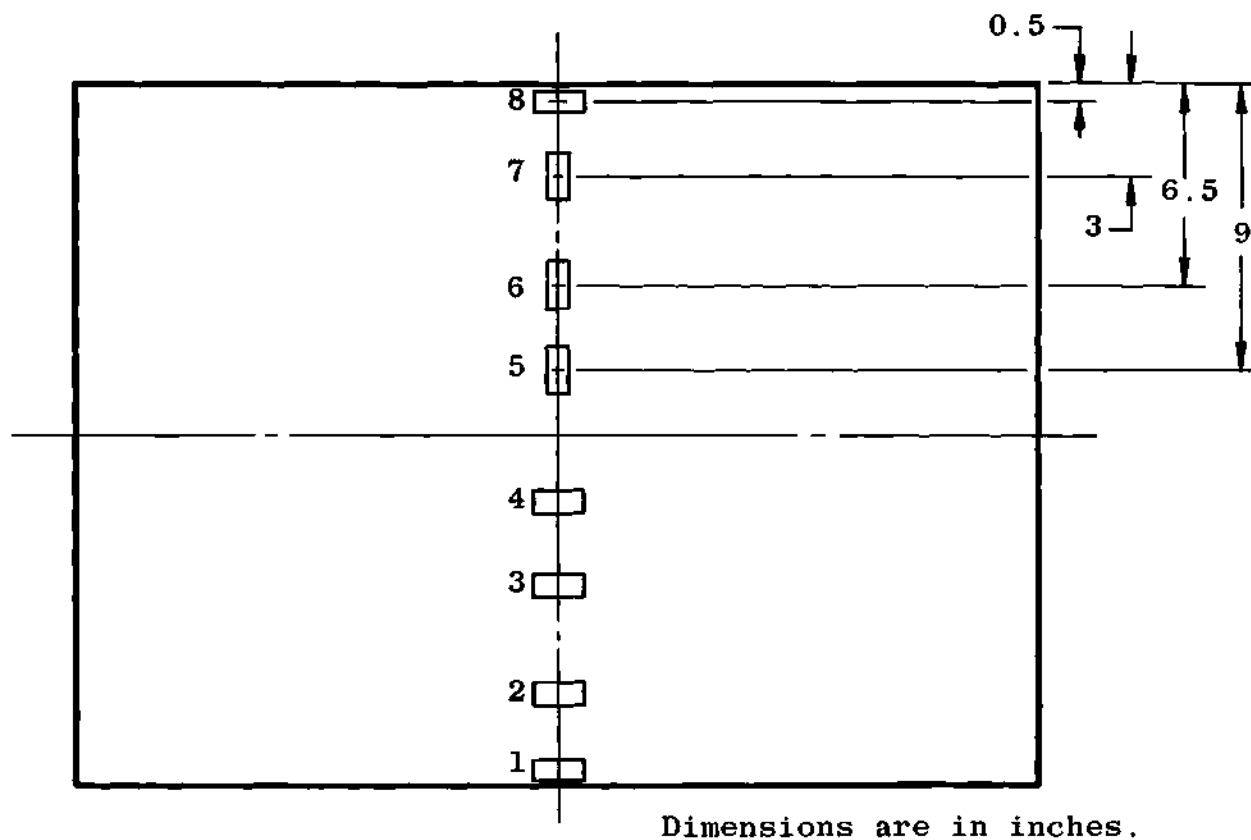
Figure 19.   Strain Gage Location on the Rectangular Plate

with Sauereisen Type 63 electric heater cement. To reduce
the effect of resistance change of the lead wires with tem-
perature, two lead wires were connected at one terminal of
the active gage and one at the other terminal. The lead
wires were arranged to keep equal lengths in the heated area
and connected so that a lead wire was in series with both
the active and dummy gages, thus effecting a temperature
compensation. An attempt was made to minimize lead wire
resistance variations between different gages by cutting all
lead wires to the same length and making all connections as
identical as possible. The dummy gage used in the circuit
was a variable resistor which proved to be more satisfactory
than either a fixed resistor or a gage, and will be discussed
further in the section on test procedure. After the instal-
lation of the strain and temperature instrumentation, the
test plate was placed in an electric oven and heated uni-
formly while the strain gages were calibrated for apparent
strain from room ambient temperature to 250°F. The average
of three calibration runs was plotted for each of the eight
gages and used for corrections to the data during the thermal-
gradient runs. Since the maximum temperatures that the gages
were subjected to were less than the manufacturer's recom-
mended maximum temperature, no correction was made for gage
factor variation.

The effect of strain-gage transverse sensitivity was
investigated, however, because the EBF-7S+ gages have wire

grids and are more sensitive to transverse strain that the foil types. Since calculations[7,8], indicated that the transverse strain on the gages would affect the readings by less than one-half per cent, no corrections were made for transverse strain.

Test Installation

The instrumented plate was installed in a specially constructed box of sufficient size to allow six inches of insulation on all sides of the plate. The heater bars were clamped to the plate longitudinal centerline with the minimum pressure required to insure good contact. The cooling water tubes which provided the heat sink were slid into snug contact with the edges of the plate.

All the instrumentation and power leads were brought out the top of the box, and it was completely filled with fine vermiculite. A Fiberglas blanket was placed over the top of the box as this was the only surface that did not have the additional insulating effect of the one-half-inch plywood box. The thermocouple leads were connected into the switching circuit junction block. The strain instrumentation leads were brought to a Baldwin SR-4 bridge switching-balancing unit, S/N 1047, which was connected to a Baldwin SR-4, type L strain indicator. This circuit·schematic is shown in Figure 20. The connection of the power leads and the cooling water tubes completed the installation.
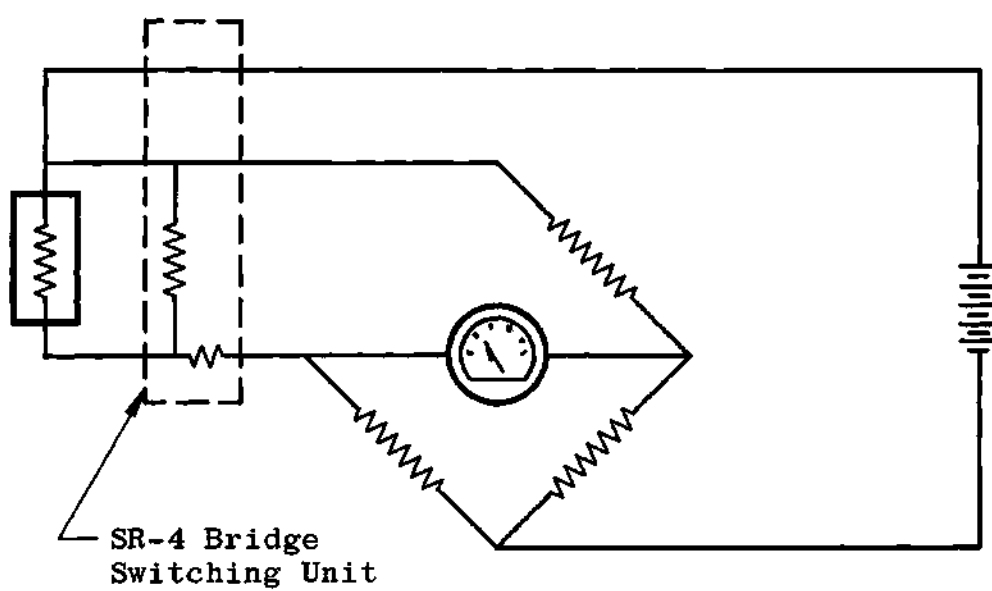
Figure 20. Schematic Drawing of the Strain
Measuring Circuit

Test Procedure

The variation in the resistance of the individual strain gages (±0.5 ohm) necessitated adjustment of the resistances in the individual gage circuits so that the gages could all be read from a common zero point on the meter. This appeared to be a simple, straightforward task, but turned out to be a lengthy procedure because of the sensitivity of the circuit. The variable resistors in the switching unit were initially set to a mid-point position. These resistors were used for very fine zero adjustments of the gages. The external variable resistor was changed very slightly while switching through the eight gages. When a position was found that appeared to be within fine adjustment range of the zero point for all gages, the external resistor was locked into position and the zero attempt was made. If the fine adjustment was insufficient to zero the gages, the external resistor was again changed a few hundredths of an ohm and the procedure repeated. This continued until all gages could be read at the common zero. This resistance was not changed throughout the test and was maintained at a constant temperature to minimize drift.

The tests were conducted by checking all temperature and strain instrumentation at ambient temperature for correct temperature indication and zero reading. The millivolt output for the desired centerline temperature was set into the temperature controller and the heating initiated. The

heating was allowed to proceed very slowly while the edges of the plate were maintained at a constant temperature. Tests were run on the plate with center-to-edge temperature differences from 20 to 65°F. When the controller had stabilized at the desired centerline temperature, plate temperature and strain readings were recorded. Figures 21 and 22 show typical temperature profiles that were measured at different values of center-to-edge temperature differences. Figures 23 and 24 show the stress values that were calculated from the strain gage readings plotted with the results of the H&R analytical solution. As will be noted from the figures, the results are plotted for a temperature profile of 50°F. It proved to be impossible to set on an exact profile and to reproduce profiles exactly. The results of several profiles were ratioed to the 50-deg. profile for a common presentation. It was found also to be impossible to obtain the 100-deg temperature profile used in the analytic solutions because the cooling tubes proved inadequate to hold the edge temperatures down.
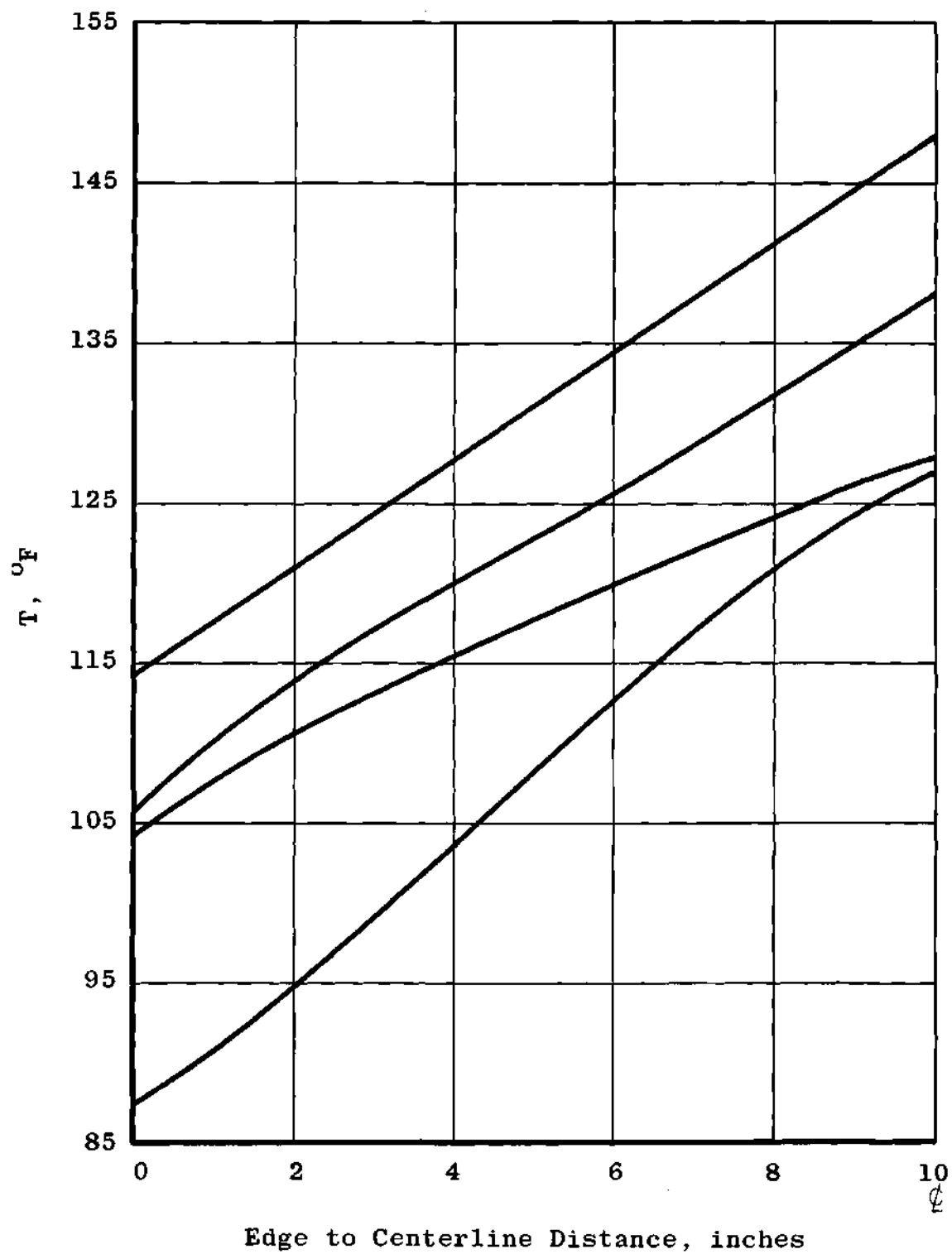
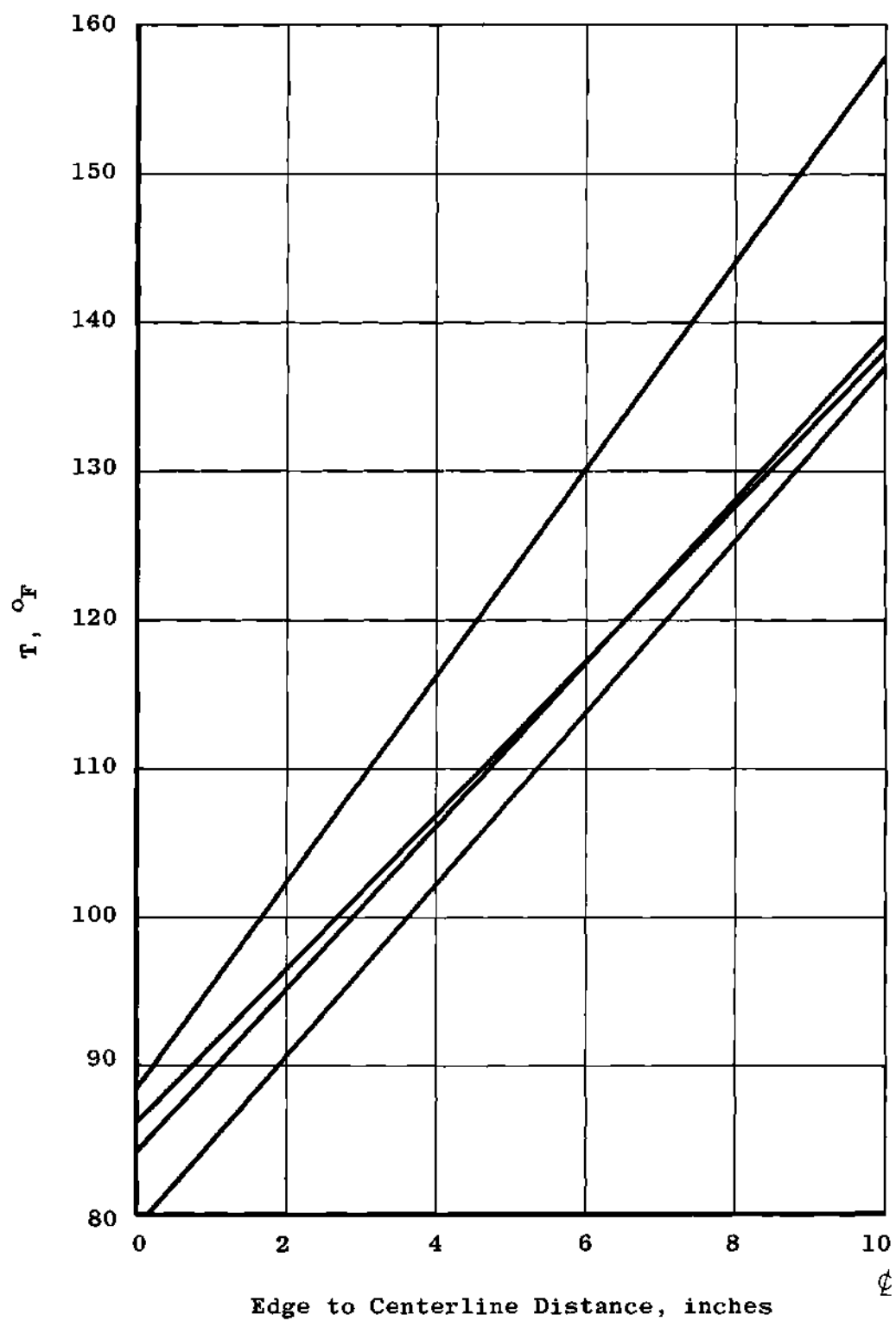Figure 21. Temperature Profiles of Rectangular
Plate, 20 to 40 Degrees

Figure 22. Temperature Profiles of Rectangular
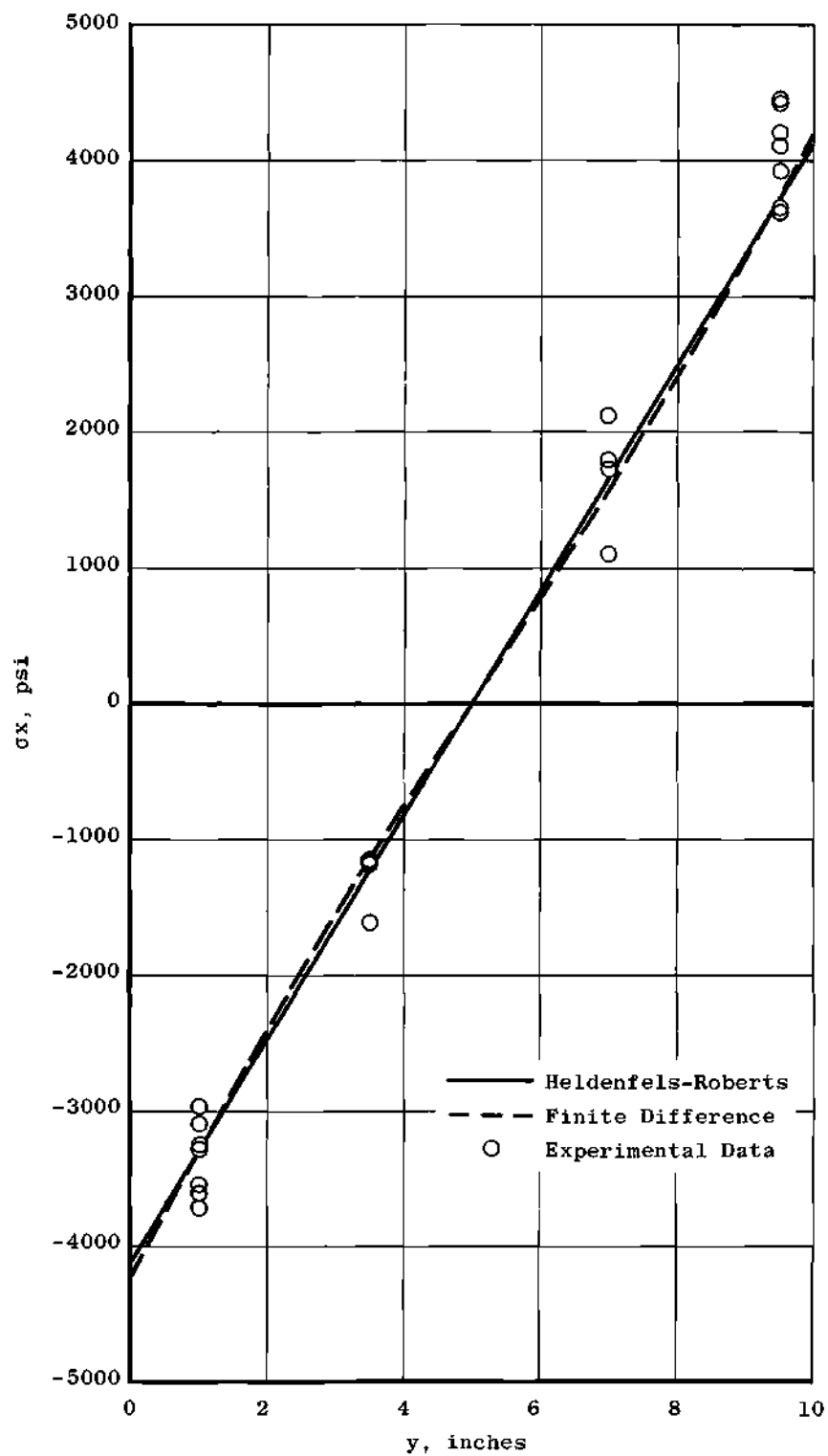Plate, 40 to 65 Degrees

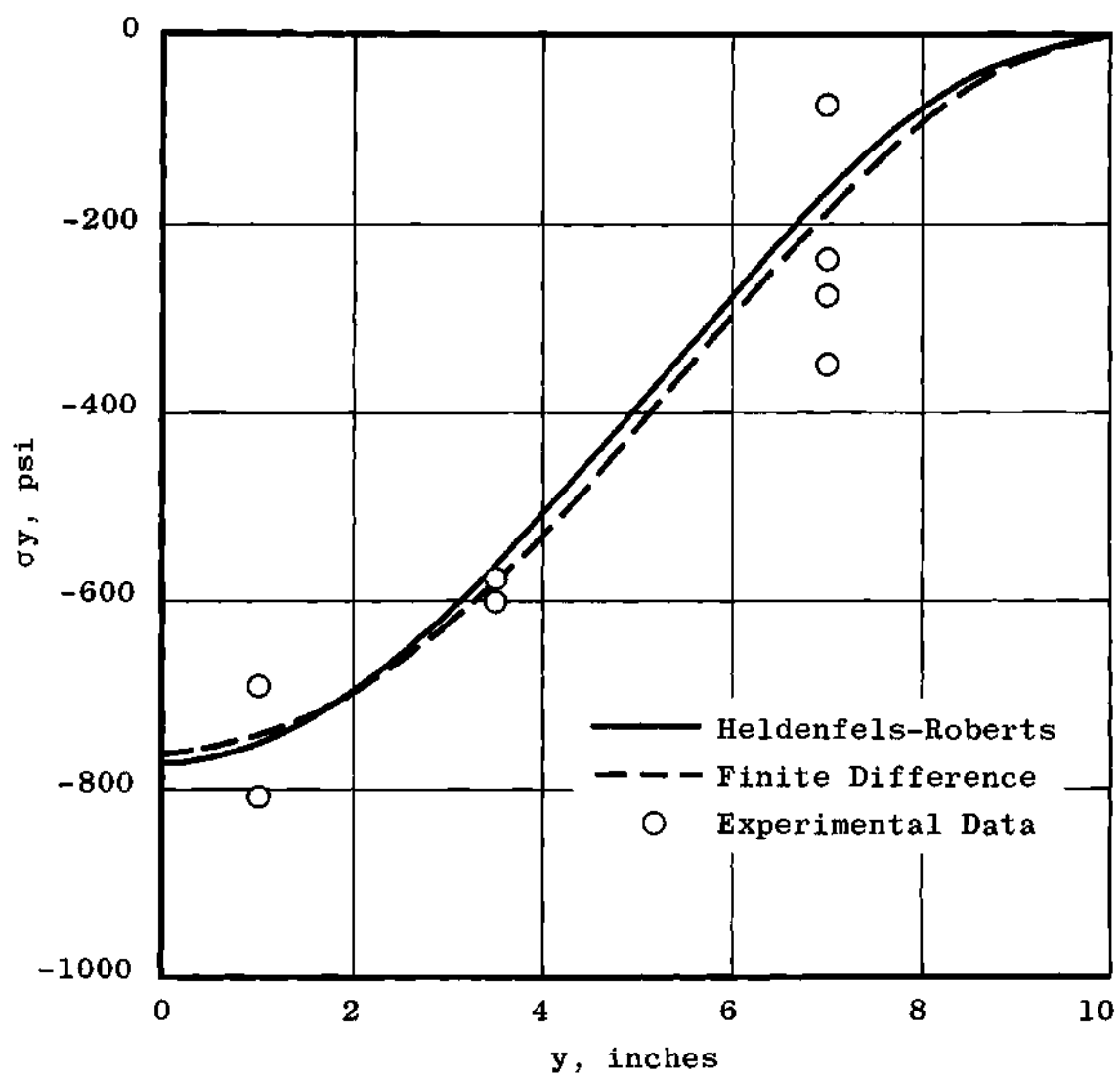Figure 23. Analytical and Experimental Stress, Transverse σx

Figure 24. Analytical and Experimental Stress, Transverse σy

CHAPTER VI

DISCUSSION

Two methods for solving two-dimensional thermal stress problems in the elastic range were investigated and compared with experimental data. The method of Heldenfels and Roberts, which is an approximate solution to the biharmonic equation, is convenient to use and gives results of acceptable accuracy. Although the equations of Heldenfels and Roberts would be difficult to use with hand calculations, they can be readily programmed for solution by digital computer and were programmed in this investigation. One reference[9] compared the method of Heldenfels and Roberts with Horvay's method of self-equilibrating polynominals. The Horvay method involves the principle of minimum complementary energy and a series solution is assumed. This solution is a function of the edge tractions applied to a section removed from an infinite plate. The two methods give solutions that are almost identical except for the end regions of the plate. This is attributed to the fact that in the Heldenfels and Roberts method it is assumed that $f(y)$ remains constant with x. It may be said of both methods that energy considerations cannot bring out local effects such as occur at corners; both methods should be taken as only approximate in regions where local effects are of importance.

The finite-difference equations, which were programmed for digital computer solution, improved with great numbers of iterations; with the largest number of iterations used in this investigation, the results were a good approximation to actual stress values. For those problems that require a numerical solution of this type, however, the Alternating Direction Method as employed by Murphy is recommended because of the more rapid convergence and shorter time required.

The results of the experimental program compared rather favorably with the analytical results. As Figures 24 and 25 indicate, there is a considerable amount of scatter, but it is fairly equally spaced around the analytical curves and does not show either a consistently high or low trend.

There are several possible explanations for the scatter. The installation of temperature-compensated strain gages is a specialized manual skill; it is known that the installation of the gages on the rectangular plate did not correspond exactly to the desired individual directions and locations. The strain-measuring circuit involved switching inside the bridge circuit, which is undesirable because of possible resistance variation across the switch contacts. The temperature profiles across the plate varied from the linear profile assumed in the analytical solutions. Referring to the typical profiles in Figures 21 and 22, the deviation can be seen. It is more pronounced at the lower ΔT than at the higher. In the analytical solutions, a steady-state

temperature field was assumed; this is extremely difficult to achieve experimentally. Finally, there was some longitudinal temperature variation. The analytical solutions assumed T to be a function of y only. This longitudinal variation was small, being in the order of $\pm 4^{O}F$ along the plate, but is could have contributed to the scatter.

This investigation proved to be extremely interesting, and it is felt that much additional work can be done in this general field with different geometrical shapes and locations of heat input.

LITERATURE CITED

1. S. Timoshenko and J. N. Goodier, Theory of Elasticity, McGraw-Hill Book Co., Inc., New York, New York (1951).

2. R. R. Heldenfels and W. M. Roberts, "Experimental and Theoretical Determination of Thermal Stresses in a Flat Plate," NACA Technical Note 2769, (August 1952).

3. K. S. Kunz, Numerical Analysis, McGraw-Hill Book Co., Inc., New York, New York (1951), p. 322.

4. V. N. Faddeeva, Translated by C. D. Benster, Computational Methods of Linear Algebra, Dover Publications, Inc., New York, New York (1959), pp. 131-143.

5. J. H. Murphy, Thermal Stresses in a Rectangular Plate, Ph.D. Thesis, Georgia Institute of Technology (September, 1962).

6. Bulletin 4310-62, "Strain Gages," Baldwin-Lima-Hamilton Corporation, Waltham, Massachusetts (1962).

7. C. C. Perry and H. R. Lissner, The Strain Gage Primer, McGraw-Hill Book Co., Inc., New York, New York (1955), p. 55.

8. Charles T. Wu, "Transverse Sensivity of Bonded Strain Gages," Journal of the Society of Experimental Stress Analysis (November, 1962), p. 338.

9. J. Singer, M. Anliker, and S. Lederman, "Thermal Stresses and Thermal Buckling," WADC Technical Report 57-69, (April, 1957), pp. 19-31.